Heliyon 10 (2024) e28719

Contents lists available at ScienceDirect

Heliyon

journal homepage: www.cell.com/heliyon

Research article

Energy efficient optimal deployment of industrial wireless mesh networks using transient trigonometric Harris Hawks optimizer

Hakim Abdulrab [a], Fawnizu Azmadi Hussin [b,*], Idris Ismail [b], Maher Assad [c], Azlan Awang [b], Hussein Shutari [b], Devan Arun [b]

[a] School of Elecetrical Engineering & Artificial Intelligence Xiamen University Malaysia, Jalan Sunsuria, Bandar Sunsuria, 43900 Sepang, Selangor, Malaysia

[b] Department of Elecetrical & Electronics Engineering Universiti Teknologi PETRONAS, Seri Iskandar, 31750, Perak, Malaysia

[c] Department of Electrical & Computer Engineering, Ajman University, Ajman, United Arab Emirates

A R T I C L E I N F O

Keywords:
WMN optimal localization
Sink node placement
Efficient energy utilization
Optimal WMN deployment
Metaheuristic algorithms, hybridization, and industrial wireless mesh networks

A B S T R A C T

Wireless mesh networks (WMNs) play a vital role in modern communication systems, and optimizing the placement of wireless mesh routers is crucial for achieving efficient network performance in terms of coverage and connectivity. However, network congestion caused by overlapping routers poses challenges in WMN optimization. To address these issues, researchers have explored metaheuristic algorithms to strike a balance between coverage and connectivity in WMNs. This study introduces a novel hybrid optimization algorithm, namely Transient Trigonometric Harris Hawks Optimizer (TTHHO), specifically designed to tackle the optimization problems in WMNs. The primary objective of TTHHO is to find an optimal placement of routers that maximizes network coverage and ensures full connectivity among mesh routers. Notably, TTHHO's unique advantage lies in its efficient utilization of residual energy, strategically placing the sink node in areas with higher energy levels. The effectiveness of TTHHO is demonstrated through a comprehensive comparison with seven well-known algorithms, including Harris Hawks optimization (HHO), Sine Cosine Algorithm (SCA), Gray Wolf Optimization (GWO), Particle Swarm Optimization (PSO), Moth Flame Optimization (MFO), Equilibrium Optimizer (EO), and Transient Search Optimizer (TSO). The proposed algorithm is rigorously validated using 33 benchmark functions, and statistical analyses and simulation results confirm its superiority over other algorithms in terms of network connectivity, coverage, congestion reduction, and convergence. The simulation outcomes demonstrate the effectiveness and efficacy of the proposed TTHHO algorithm in optimizing WMNs, making it a promising approach for enhancing the performance of wireless communication systems.

1. Introduction

Wireless Mesh Networks (WMNs) have emerged as a promising solution for providing ubiquitous and high-speed connectivity in various domains, ranging from urban environments to rural areas [1]. These networks consist of interconnected mesh nodes that collaborate to relay data and extend the coverage area. However, the efficient deployment of WMNs poses several challenges, such

* Corresponding author.
E-mail address: fawnizu@utp.edu.my (F.A. Hussin).

https://doi.org/10.1016/j.heliyon.2024.e28719
Received 3 September 2023; Received in revised form 12 March 2024; Accepted 22 March 2024

Available online 27 March 2024

as optimizing energy consumption, ensuring optimum coverage, and establishing reliable connectivity [2,3]. Despite the numerous advantages presented by Wireless Mesh Networks (WMNs), certain issues persist that demand resolution to strengthen network performance. These concerns incorporate aspects such as coverage, connectivity, congestion, compatibility, security, etc [4]. The deployment of WMNs involves determining the optimal placement of mesh nodes to ensure efficient network operation [5]. One of the key objectives is to minimize the energy consumption of the network since wireless mesh nodes are often battery-powered and energy-constrained [6]. By strategically deploying nodes, unnecessary energy expenditure can be avoided, thereby prolonging the network's lifetime [7].

Moreover, achieving optimum coverage is crucial to ensure that the network can serve the intended area effectively. The coverage of a WMN refers to the ability of the network to provide reliable and uninterrupted connectivity to all desired locations [8]. In addition to coverage, establishing robust connectivity is essential for a WMN's performance which refers to the ability of mesh nodes to ensure and maintain reliable communication links with each other [9]. A well-connected network enhances data transmission efficiency, improves fault tolerance, and enables efficient routing. Therefore, it is important to deploy mesh nodes in such a way that signal strength and quality are sufficient to support communication throughout the coverage area, while minimizing the number of nodes required [10].

Optimally deploying routers in an energy-efficient manner while ensuring both optimal coverage and connectivity is a complex optimization problem that needs to be effectively addressed. One viable option is through utilizing meta-heuristic algorithms, which can provide a means to intelligently explore the vast solution space of WMN deployment, considering various constraints, objectives, and trade-offs. These algorithms are iterative and heuristic-based approaches that employ exploration and exploitation techniques to search for optimal or near-optimal solutions [11,12]. By evaluating different node placement configurations and iteratively refining them, these algorithms can converge towards solutions that optimize energy consumption while ensuring adequate coverage and connectivity [13,12,14].

In this context, numerous studies have employed meta-heuristic algorithms to address WMNs placement issues. However, some of these studies have relied on a single algorithm, which is inherently limited. Single algorithms can become trapped in local optima, lack adaptability in response to changing conditions, and struggle to effectively utilize problem-specific knowledge. In addition, some studies have solely focused on coverage and connectivity, often overlooking the crucial factor of energy consumption, which should be a core consideration throughout the placement process to ensure the network's long-term sustainability and effectiveness. This serves as the primary motivation for the development of new hybrid optimization approaches that combine the complementary strengths of multiple meta-heuristic algorithms. Hybrid algorithms aim to achieve better optimization performance leading to more optimal and effective wireless network deployments. This research work initially conducts comprehensive evaluations of some well-known meta-heuristic algorithms, comparing their performance in terms of energy efficiency, coverage, and connectivity metrics. Simulations are conducted on WMN scenarios, considering various network typologies. Hence, the results are to provide valuable insights into the strengths and weaknesses of each algorithm and guide the selection of the most suitable algorithm for specific deployment scenarios.

By leveraging metaheuristic algorithms, such as Transient Search Optimizer (TSO) [15], Harris Hawks Optimization (HHO) [16] and Sine Cosine Algorithm (SCA) [17], it is possible to find solutions that balance the trade-off between energy consumption and network performance. These algorithms can intelligently explore the search space and adaptively refine the mesh node placement, considering various constraints and objectives. This paper makes original and significant contributions in this field, as summarized below:

- A new optimization technique called Transient Trigonometric Harris Hawks Optimizer (TTHHO) has been proposed for tackling WMN issues such as connectivity, coverage, congestion reduction and energy-based optimal sink nod placement.
- The performance evaluation of TTHHO involved testing it on 33 benchmark functions and the WMN model. To ensure a fair comparison among all investigated algorithms, modified versions of standard optimization algorithms with a local search improvement mechanism were utilized.
- A noteworthy interdisciplinary accomplishment in wireless communication, optimization, and industrial planning is achieved through the optimized placement of routers in WMN using TTHHO. This significantly improves connectivity and coverage.
- This work also includes the proposal of an efficient energy-based optimal sink node placement to increase the lifetime of WMN.
- Additionally, TTHHO yields cost reduction and substantial improvement in network congestion by requiring fewer node placements compared to other algorithms. Remarkably, the reduced number of nodes does not compromise TTHHO's ability to create a reliable WMN with full coverage and connectivity.

The remainder of this article as structured as follows: Section 2 provides insights about optimal nodes placement strategies and WMN optimization using metaheuristic algorithms. Section 3 covers the proposed approach hierarchical design associated with the mathematical modeling of the optimization search strategies and the proposed fitness functions. Results and discussion are then covered in Section 4. Lastly, Section 5 concludes the overall view of this article.

2. Literature review

Although meta-heuristic optimization methods are limited to finding local optimal solutions, they have been widely developed and achieved greater success than other techniques. In most practical situations, meta-heuristic techniques are able to discover the most suitable and dependable network design to address mesh router placement problems.

Previous studies, such as those conducted by [18] and [19], primarily focused on placing wireless routers in frequent network areas but overlooked the deployment of mesh routers. In contrast, some other research considered a continuous deployment region, offering more flexibility in mesh router placement and resulting in better network design. These studies also delved into the use of hierarchical optimization techniques to enhance network connection and client coverage. However, they found that this approach was not suitable for achieving non-convex goals, as evidenced by research conducted by [20], [21], and [22].

Numerous studies have employed various meta-heuristic techniques to improve client coverage and network connectivity, as exemplified in [19] and [23]. In the work by [23], a simulation system based on Hill Climbing (HC) and Simulated Annealing (SA) was developed to tackle the node placement problem in WMNs. On the other hand, [19] utilized the Tabu Search (TS) algorithm for optimizing node deployment solutions. The results exhibited superior performance by TS compared to the Simulated Annealing (SA) method. Furthermore, in a study by [24], the authors utilized the Friedman test to evaluate and compare the performance of several meta-heuristic algorithms, including genetic algorithm, tabu search, hill-climbing, and simulated annealing.

The PSO metaheuristic has been successfully employed to tackle the router node placement problem in WMNs, aiming to optimize network connection and client coverage, as detailed in [25] and [26]. These studies have investigated various factors that influence the performance of the PSO algorithm, including network design characteristics. In [25], the authors proposed a method to assign a digit to each mesh network client, indicating its service priority. Moreover, the work in [27] adopted Bat-inspired methods, incorporating client motion while maintaining service priorities. The study in [26] introduced a PSO technique that incorporates social cognition for dynamic WMNs. The wireless mesh network-router node placement (WMN-RNP) was made as a dynamic configuration with a combined objective function. Authors in [20] employed the simulated annealing algorithm that weighed momentum needs to solve the service prioritization problem in WMNs. Authors in [28] developed an electromagnetism-like algorithm to maximize network connectivity and client coverage in WMNs.

Several effective population-based algorithms used for optimal network placement in FiWi networks include Slime Mould Algorithm (SMA) [29], Weighted Salp Swarm Algorithm (WSSA) [30], Chaotic Local Search-based Levy Flight Distribution (CLS-LFD) [31], Enhanced Backtracking Search Algorithm (EBSA) [32], and Marine Predators Algorithm (MPA) [33]. In their research, Singh and Prakash [34] explored the optimal placement of relay nodes in fiber-wireless networks. They utilized Whale Optimization approach (WOA) to determine the most favorable positioning of Optical Network Units (ONUs) taking into account the distribution of mesh routers and ONUs. The study also compared the results of the WOA approach with those of the Moth Flame Optimizer (MFO) and Greedy methods. In a different study conducted by Gupta and Jha [35], the authors applied a Biogeography-Based Optimization (BBO) algorithm to optimize the placement of sensor devices in a sensor network. The objective was to achieve m-connectivity and k-coverage. Both of these studies focus on optimizing the placement of relay nodes in wireless networks. The primary benefits of these algorithms are their low computational demands, rapid convergence, and independence from prior knowledge. However, challenges such as getting stuck in local optima and the necessity of tuning parameters are notable drawbacks of these population-based meta-heuristics.

Nitesh and Jana's work [40] aims to minimize network costs by reducing the number of relay nodes required while still maintaining k-coverage and s-connectivity. They achieve this by minimizing the amount of overlapping coverage between relay nodes. On the other hand, the study by Sapre and Das [41] uses the MFO algorithm to ensure complete connectivity between all nodes in the network. The focus is on maximizing network connectivity rather than minimizing costs. Both approaches are important considerations when optimizing relay node placement in wireless networks. Furthermore, Nitesh and Jana proposed a method to position relays in their study published in [40]. Their approach guaranteed both s-connectivity among the relays and k-coverage of the deployment region. To minimize network costs, their method utilized fewer relay nodes by reducing the amount of overlapping coverage between them. On the other hand, the MFO algorithm was employed by Sapre and Sahu in [41] to determine the optimal locations for placing the nodes. The primary objective was to ensure that all parts of the network were connected, and the technique used a fully connected network heuristic to assess network connectivity.

Table 1 outlines some of the previous researches on the WMN placement approaches. The study described in [3] utilized a unique version of the HHO to efficiently place mesh routers within WMN, resulting in improved connectivity and coverage for various network sizes. Through statistical analyses and simulation results, HHO was found superior to other bechmarking algorithms. Although previous research has confirmed the effectiveness of the HHO, there are still issues with premature convergence and being trapped in local best solutions. Consequently, researchers from different fields have developed various modified and hybrid algorithms to overcome these problems.

The SCA, developed by Seyedali Mirjalili in 2016 [17], is an efficient optimization algorithm to that can be utilized overcome HHO drawbacks. Due to its favorable properties, the SCA has been successfully applied in various fields, such as feature selection [42], wind power control [43,44], machine learning [45]. Additionally, the SCA has been hybridized with the TSO and arithmetic optimization algorithm (AOA) as in [46,47].

Building upon these advancements, the authors of [48] developed a hybrid optimization algorithm called Hybrid Harris Hawk Optimization and Sine Cosine Algorithm (HHOSCA). By combining the strengths of both algorithms, HHOSCA aims to further improve optimization performance and address complex problems effectively. However, the lack of full coverage in [48] may result in areas with limited or no access, compromising the overall effectiveness of the network. Moreover, energy efficiency is a critical factor in WMN design, as the limited energy resources of individual routers directly impact the network's longevity and sustainability. To address these limitations, the proposed TTHHO algorithm in this study provides a holistic approach to WMN optimization. By strategically placing routers based on efficient residual energy and considering coverage as a primary objective, TTHHO aims to achieve full coverage while simultaneously maximizing network connectivity and energy efficiency.

Table 1
Some existing researches on WMN router placement.

Ref. Year	Algorithm	Addressed Issues	Advantages	Limitations
[19] 2015	TS	WMN connectivity and coverage.	- Adopting TS algorithm to solve WMN router deployment. - Avoiding repetition of solved placements using memory based techniques.	- The approach primarily emphasized improving network connectivity, but it resulted in inadequate user coverage.
[26] 2016	PSO	WMN connectivity and coverage.	-Incorporating the dynamics of social community behavior. -Improving the connectivity of the network. -Expanding the network's coverage in social contexts.	-The mesh routers have limitations in terms of serving a defined number of clients. -This work is deficient in optimizing the residual energy consumption.
[36] 2020	SA	WMN connectivity, cost, and coverage.	-Introduction of a novel SA-based Center of Mass (SAC) method. -Achieving quicker convergence in contrast to traditional SA. -Elevating network quality and performance.	-The study has not tackled the issue of network connectivity. -The challenges posed by harsh environments have not been taken into account.
[37] 2020	HHO	Sink node placement.	-Introducing an approach to determine the optimal sink node placement. -Employing HHO algorithm to find the optimal placement of sink node.	- The work did not address coverage and connectivity issues in WMNs. -The issue of congestion in WMN was not addressed in this research
[38] 2021	PSO	WMN connectivity and coverage.	-Creating an Accelerated PSO (APSO) framework. -Streamlining complexity and enhancing efficiency in comparison to LDWPSO.	-The research has made notable enhancements in network connectivity, but the issue of coverage remains unresolved. -The validation was conducted using a single algorithm, which may not be sufficient to establish its superiority comprehensively.
[18] 2022	MVOA	WMN connectivity and coverage.	-Introducing novel criteria for network evaluation, taking into account the ratio of active clients to routers. -Decreasing path-losses and elevating connectivity in comparison to GA, WOA, and PSO.	-The optimization of network coverage has not been adequately addressed in this work. -This research did not investigate efficient energy consumption in any depth.
[39] 2022	COA	WMN connectivity and coverage.	-Employing COA for addressing router deployment challenges. -Evaluating the effectiveness of COA through comparisons with various algorithms in addressing optimization problems.	-This study did not explore the optimization of sink localization. -Additionally, it did not incorporate energy consumption optimization into its analysis.
[3] 2022	HHO	WMN connectivity and coverage.	- An innovative utilization of HHO in WMNs -Enhancing network connectivity and coverage. -Conducting a range of statistical analyses to demonstrate the improvements	-This research lacks the mitigation of network congestion. -It is also deficient in optimizing the residual energy consumption.

3. Methodology and system model

In this section, an elaboration on the method used to optimize the coverage, connectivity, and reduce network congestion in a wireless network is provided. The main focus of this work is to develop a hybrid optimization technique known as Transient Trigonometric Harris Hawks Optimizer (TTHHO). The objective is to minimize network congestion while significantly improving the coverage and connectivity of WMN. Furthermore, an important aspect of the proposed method is to create an energy-efficient WMN by optimizing the placement of sink nodes. By strategically positioning sink nodes, the network's overall energy consumption can be minimized, leading to a more sustainable and efficient WMN. In addition, this section also covers the hierarchical design, mathematical modeling, and fitness functions employed in the optimization process.

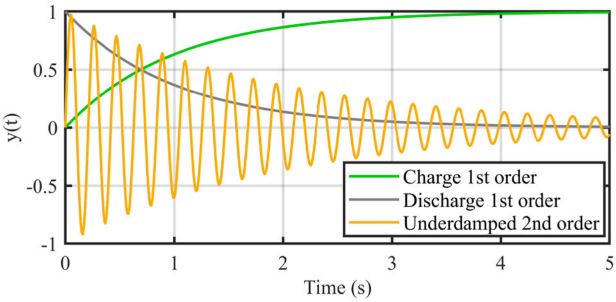

Fig. 1. RCL various order system response.

3.1. Transient search optimizer

The TSO algorithm follows a three-stage process, including initialization, exploration, and exploitation, to optimize the search process. During initialization, search-agents are randomly generated within specified bounds. The algorithm's exploration behavior is inspired by the oscillations of second-order RLC circuits around the zero point, while the exploitation phase draws from the exponential decay observed in first-order discharging circuits. Fig. 1 shows the response of RLC for various system order. Balancing exploration and exploitation is achieved using a random number (r_7), where $r_7 \geq 0.5$ emphasizes exploration, and $r_7 < 0.5$ shifts the focus to exploitation. The mathematical modeling of TSO's exploitation and exploration is illustrated by Eq. (3), that is influenced by Eqs. (1) and (2). The TSO's favorite solution (y_{best}) replicates the electrical circuit's final value or steady state ($x(\infty)$).

$$y(t) = y(\infty) + (y(0) - y(\infty))e^{\frac{-t}{\tau}} \tag{1}$$

where t represents time, $y(t)$ corresponds to either the capacitor voltage $v(t)$ of the RC circuit or the inductor current $i(t)$ of the RL circuit. τ denotes the time constant of the circuit, which is equivalent to the product of the resistance (R) and capacitance (C) in the RC circuit, given by $\tau = RC$.

$$y(t) = e^{-\alpha t}(B_1 cos(2\pi f_d t) + B_2 sin(2\pi f_d t)) + y(\infty) \tag{2}$$

where α is the damping coefficient, f_d is the damped resonant frequency, and B_1 and B_2 are constants.

$$y_{t+1} = \begin{cases} y_{best} + (y_t - C_1 * y_{best}) * e^{-L}, \; r_7 < 0.5 \\ y_{best} + e^{-L}[cos(2\pi L) + sin(2\pi L)] * |y_t - \\ \quad C_1 * y_{best}|, \; r_7 \geq 0.5 \end{cases} \tag{3}$$

3.2. Proposed transient trigonometric Harris Hawks optimizer

While the previously developed HHOSCA [48] demonstrates commendable performance, it still exhibits certain limitations, including premature convergence and the struggle to reach global optima. To overcome these shortcomings, we propose a novel approach known as Transient Trigonometric Harris Hawks optimizer (TTHHO), which integrates the strengths of HHO, SCA, and TSO. The aim is to enhance the convergence behavior and solution quality. By employing a hybrid method, the TTHHO approach is expected to produce more diverse solutions, as it can make significant jumps within the search zone at frequent intervals to avoid getting stuck at a local optimum. This increased exploration capability allows for the generation of more varied solutions, thus making the search process more effective and adequate.

Fig. 2 illustrates the hierarchical configuration of the proposed TTHHO algorithm, with distinct layers responsible for specific tasks. The bottom layer, represented by TSO, is responsible for updating the individuals generated by SCA in the middle layer. Subsequently, the HHO-generated top-layer individuals are kept up-to-date by SCA. In this hierarchical design, the top-layer comprises M searching agents, which correspond to M groups in the middle layer, where each group contains N SCA population. Similarly, the bottom-layer consists of O TSO populations. The optimization process commences with executing SCA and TSO on the middle and bottom layers to update the positions of individuals. The best solution identified by each group in the bottom and middle layers is retained by their corresponding agent in the top layer. Utilizing this best solution, the positions of HHO individuals in the top layer are updated, generating new equations that represent the exploitation and exploration phases. This hierarchical approach fosters effective cooperation among the different components, leading to notable improvements in solution quality and convergence behavior.

The arithmetic equation (4) represents the model of exploration phase of the TTHHO in which the escaping energy of the prey is greater or equal to $|E| \geq 1$. Prey's energy is inspired by Harris Hawks hunting habits. For simplicity, the mathematical models of the behavior occurred at the bottom and middle layers are represented by the symbols A, B, C and D as in (5). Some of the parameters are defined in (6) where t and T represent the current iteration and the maximum number of iterations, respectively.

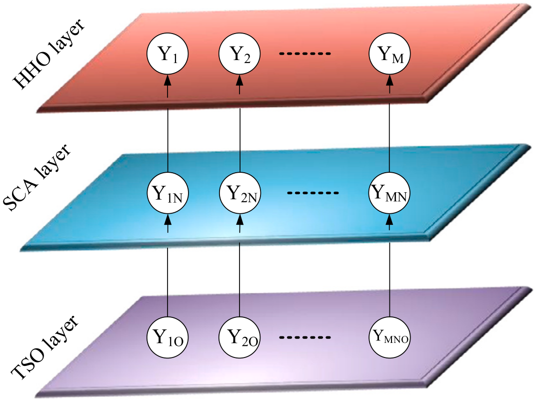

Fig. 2. The proposed TTHHO hierarchical structure.

$$y_{t+1} = \begin{cases} y_{rand} - r_1 * \left|y_{rand} - 2 * r_2 * [A]\right|, \quad r_3 < 0.5, \\ \qquad r_7 < 0.5 \text{ and } q < 0.5 \\ y_{rand} - r_1 * \left|y_{rand} - 2 * r_2 * [B]\right|, \quad r_3 < 0.5, \\ \qquad r_7 \geq 0.5 \text{ and } q < 0.5 \\ y_{rand} - r_1 * \left|y_{rand} - 2 * r_2 [C]\right|, \quad r_3 \geq 0.5, \\ \qquad r_7 < 0.5 \text{ and } q < 0.5 \\ y_{rand} - r_1 * \left|y_{rand} - 2 * r_2 [D]\right|, \quad r_3 \geq 0.5, \\ \qquad r_7 \geq 0.5 \text{ and } q < 0.5 \\ \left[y_{best} - Y_m\right] - r_1 * \left(r_2(u_b - l_b) + lb\right), \quad q \geq 0.5 \end{cases} \tag{4}$$

$$\begin{aligned} &A = y_{best} + \left(y_t - C_1 * y_{best}\right)e^{-L} + r_1 \sin\left(r_5\right) \times \Big|r_6 * y_{best} - \left(y_{best} + \left(y_t - C_1 * \right.\right. \\ &\left.\left. y_{best}\right)e^{-L}\right)\Big| \\ &B = y_{best} + e^{-L}\left[\cos\left(2\pi L\right) + \sin\left(2\pi L\right)\right]\left|y_t - C_1 * y_{best}\right| + r_1 \sin\left(r_5\right) \times \Big|r_6 * \\ &y_{best} - \left(y_{best} + e^{-L}\left[\cos\left(2\pi L\right) + \sin\left(2\pi L\right)\right]\left|y_t - C_1 * y_{best}\right|\right)\Big| \\ &C = y_{best} + \left(y_t - C_1 * y_{best}\right)e^{-L} + r_1 \cos\left(r_5\right) \times \Big|r_6 * y_{best} - \left(y_{best} + \left(y_t - C_1 * \right.\right. \\ &\left.\left. y_{best}\right)e^{-L}\right)\Big| \\ &D = y_{best} + e^{-L}\left[\tan\left(2\pi L\right) + \sin\left(2\pi L\right)\right]\left|y_t - C_1 * y_{best}\right| + r_1 \cos\left(r_5\right) \times \Big|r_6 * \\ &y_{best} - \left(y_{best} + e^{-L}\left[\tan\left(2\pi L\right) + \sin\left(2\pi L\right)\right]\left|y_t - C_1 * y_{best}\right|\right)\Big| \end{aligned} \tag{5}$$

$$\begin{aligned} &E_1 = 2 * (1 - \frac{t}{T}) \\ &L = 2 * r_1(1 - E_1) \\ &C_1 = K * r_2 * E_1 + 1 \\ &E_0 = 2 * r_1 - 1 \\ &E = E * E_0 \\ &r_5 = 2\pi * rand() \\ &r_6 = 2 * rand() \\ &K = 1 \\ &J = 2(1 - r_1) \end{aligned} \tag{6}$$

where r_1, r_2, r_3, r_4, r_7, and q are random parameters distributed uniformly $\in$ [0,1], y_{best} is the transient best solution obtained so far, y_t is the current solution, Y_m is the average mean of the population, and u_b and l_b are the upper and lower bounds, respectively.

Likewise HHO, the TTHHO performs the exploitation phase by applying the besieging strategies. They are categorized into hard besiege, hard besiege with progressive quick dives, soft besiege and soft besiege with progressive quick dives. Switching between these strategies is determined by the escaping energy level of the prey ranging within $E \in [0, 1]$ and the value of the randomly generated parameter $r \in [0, 1]$. The mathematical representation of these strategies is further elaborated in the following formulas:

- **Hard besiege**: The inspiration of the hawk's natural behavior where it targets the prey which has less energy to be able to flee the hunt. In this hybrid method, the arithmetic equation that represents this behavior is given in (7) with the condition of $E < 0.5$ and $r \geq 0.5$.

$$y_{t+1} = \begin{cases} y_{prey} - E * \left| y_{prey} - 2 * r_2 * [A] \right|, r_3 < 0.5 \\ \quad and\ r_7 < 0.5 \\ y_{prey} - E * \left| y_{prey} - 2 * r_2 * [B] \right|, r_3 < 0.5 \\ \quad and\ r_7 \geq 0.5 \\ y_{prey} - E * \left| y_{prey} - 2 * r_2 * [C] \right|, r_3 \geq 0.5 \\ \quad and\ r_7 < 0.5 \\ y_{prey} - E * \left| y_{prey} - 2 * r_2 * [D] \right|, r_3 \geq 0.5 \\ \quad and\ r_7 \geq 0.5 \end{cases} \tag{7}$$

where y_{prey} denotes the preys best location and y_{best} represents the transient best solution.

- **Tough besiege with progressive fast dives**: This occurs when $r < 0.5$ and $E < 0.5$. In this scenario, the search agents demonstrate a behavior characterized by reduced exploration and increased exploitation, as they focus on locating and capturing the remaining prey with higher energy levels. This phase of the algorithm search is modeled by (8).

$$Y_{t+1}^{i} = \begin{cases} Z \ \text{if} \ F(Z) < F\left(y_t\right) \& \\ y_t = \begin{cases} A,\ r_3 < 0.5\ and\ r_7 < 0.5 \\ B,\ r_3 < 0.5\ and\ r_7 \geq 0.5 \\ C,\ r_3 \geq 0.5\ and\ r_7 < 0.5 \\ D,\ r_3 \geq 0.5\ and\ r_7 < 0.5 \end{cases} \\ X\ if\ F(X) < F\left(y_t\right) \& \\ y_t = \begin{cases} A,\ r_3 < 0.5\ and\ r_7 < 0.5 \\ B,\ r_3 < 0.5\ and\ r_7 \geq 0.5 \\ C,\ r_3 \geq 0.5\ and\ r_7 < 0.5 \\ D,\ r_3 \geq 0.5\ and\ r_7 < 0.5 \end{cases} \end{cases} \tag{8}$$

where

$$\begin{aligned} & Z = (S \times LF(d)) + X \\ & X = y_{\text{prey}} - E \left| J * y_{\text{prey}} - Y_m \right| \\ & S = 1 \times d \ \ \text{Random} \ \ \text{vector} \\ & d = \text{Dimension} \end{aligned} \tag{9}$$

$$LF(D) = \frac{\beta \times u}{|v|^{\frac{1}{\sigma}}} \times 0.01 \tag{10}$$

$$\beta = \left(\frac{\sin\left(\frac{\pi\sigma}{2}\right) \times \Gamma(1+\sigma)}{\Gamma\left(\frac{1+\sigma}{2}\right) \times \sigma \times 2^{\left(\frac{\sigma-1}{2}\right)}} \right) \tag{11}$$

where u, v denote random variables ranging from 0 to 1, σ denotes a 1.5 constant value.

- **Soft besiege**: The TTHHO employs this strategy when $E \geq 0.5$ and $r \geq 0.5$. The model of this phase is represented by (12).

$$y_{t+1} = \begin{cases} y_{prey} - [A] - E \left| J * y_{prey} - 2 * r_2 * [A] \right|, \\ \quad r_3 < 0.5\ and\ r_7 < 0.5 \\ y_{prey} - [B] - E \left| J * y_{prey} - 2 * r_2 * [B] \right|, \\ \quad r_3 < 0.5\ and\ r_7 \geq 0.5 \\ y_{prey} - [C] - E \left| J * y_{prey} - 2 * r_2 * [C] \right|, \\ \quad r_3 \geq 0.5\ and\ r_7 < 0.5 \\ y_{prey} - [D] - E \left| J * y_{prey} - 2 * r_2 * [D] \right|, \\ \quad r_3 \geq 0.5\ and\ r_7 \geq 0.5 \end{cases} \tag{12}$$

Table 2
Parameters setup of bench-marking algorithms.

Algorithm	Parameter	Value
TTHHO	Transient initializer	0
	Initial energy E_0	[-1 1]
	Escaping energy r	[0 1]
	Default constant σ	1.5
	Convergence parameter a	2
PSO	Inertia factor	0.3
	c_1	1
	c_2	1
SCA	Convergence parameter a	2
GWO	Convergence parameter a	[2 0]
EO	r	0.5
	a	4
	GP	0.5
MFO	Convergence parameter r	[-1 -2]
TSO	k	0
	Convergence parameter a	[2 0]
HHO	initial energy E_0	[-1 1]
	default parameter β	1.5
	escaping energy r	[0 1]

Table 3
Characteristic parameters of the WMN.

Parameter	Value	Initial value
Transmission range	$[20, 120]$	20 meter
Number of clients	100	100
Number of routers	$[60, 160]$	60
Area height	1000 m	1000 m
Area width	1000 m	1000 m
Residual Energy	[50,2000]	50 Joule

- **Soft besiege with progressive quick dives**: When the prey possesses sufficient energy ($E \geq 0.5$) to escape, the TTHHO employs a "soft besiege" strategy with $r < 0.5$. In this scenario, the hawk approaches the prey cautiously, allowing some space for the prey to potentially evade the attack. This behavior is modeled by (13) and (14).

$$Y_{t+1}^{i} = \begin{cases} Z \text{ if } F(Z) < F\left(y_t\right) \& \\ y_t = \begin{cases} A, \ r_3 < 0.5 \ and \ r_7 < 0.5 \\ B, \ r_3 < 0.5 \ and \ r_7 \geq 0.5 \\ C, \ r_3 \geq 0.5 \ and \ r_7 < 0.5 \\ D, \ r_3 \geq 0.5 \ and \ r_7 < 0.5 \end{cases} \\ X \ if \ F(X) < F\left(y_t\right) \& \\ y_t = \begin{cases} A, \ r_3 < 0.5 \ and \ r_7 < 0.5 \\ B, \ r_3 < 0.5 \ and \ r_7 \geq 0.5 \\ C, \ r_3 \geq 0.5 \ and \ r_7 < 0.5 \\ D, \ r_3 \geq 0.5 \ and \ r_7 < 0.5 \end{cases} \end{cases} \tag{13}$$

where

$$\begin{aligned} Z &= (S \times LF(d)) + X \\ X &= y_{\text{prey}} - E\left|J * y_{\text{prey}} - y_t\right| \end{aligned} \tag{14}$$

The working principle of the proposed TTHHO for optimizing WMN is further clarified by the mean of Pseudo code. The Algorithm 1 details out the optimization process of WMN.

3.3. Simulation configuration setup

MATLAB 2022a was used on a computer running Windows 11 to implement all of the algorithms including HHO, PSO, GWO, SCA, MFO, EO, TSO, and the proposed TTHHO. The PC had an Intel(R) Core(TM) i7-8700 processor, 32 GB of RAM, and a clock speed of 3.20 GHz. To ensure a fair comparison, all algorithms were executed with the same swarm size and number of iterations. The performance of each optimizer was recorded over 30 separate runs, and the average results were used for the comparative analysis. This thorough evaluation process enabled a comprehensive assessment of the algorithms' efficiency in optimizing the WMN.

Algorithm 1 Transient Trigonometric Harris Hawks Optimizer (TTHHO).

Input: A WMN that is comprised of mesh routers randomly positioned, and the positions of mesh clients are predetermined.
Output: Full coverage of mesh clients and fully connected mesh routers.

Initialize the positions of mesh routers randomly, y_i^0 ($i = 1, 2, 3, ..., \mathrm{N}$)
Start the iterations at $t = 1$ and set T = maximum iterations
while ($t \leq \mathrm{T}$) **do**
  Using the proposed fitness function, obtain the initial solution y_{prey} at Top layer and y_{best} at middle and bottom layers.
  for (each hawk(y_i)) **do**
    Adjust the MRs position.
    Update E Using (6)
    STARTING with EXPLORATION
    Condition at Top layer
    if $|E| \geq 1$ **then**
      if $q < 0.5$ **then**
        Condition at Bottom and Middle layers
        if $r_3 < 0.5$ and $r_7 < 0.5$ **then**
          Update the MRs locations using case 1 of (4).
        else if $r_3 < 0.5$ and $r_7 \geq 0.5$ **then**
          Update the MRs locations using case 2 of (4).
        else if $r_3 \geq 0.5$ and $r_7 < 0.5$ **then**
          Update the MRs locations using case 3 of (4).
        else if $r_3 \geq 0.5$ and $r_7 \geq 0.5$ **then**
          Update the MRs locations using case 4 of (4).
        end if
      else if $q \geq 0.5$ **then**
        Update the MRs locations using case 5 of (4).
      end if
    end if
    EXPLOITATION
    Condition at Top layer
    if $|E| < 1$ **then**
      if ($|E| < 0.5$ and $\mathrm{r} \geq 0.5$) **then**
        Condition at Bottom and Middle layers
        if $r_3 < 0.5$ and $r_7 < 0.5$ **then**
          Update the MRs locations using case 1 of (7)
        else if $r_3 < 0.5$ and $r_7 \geq 0.5$ **then**
          Update the MRs locations using case 2 of (7)
        else if $r_3 \geq 0.5$ and $r_7 < 0.5$ **then**
          Update the MRs locations using case 3 of (7)
        else if $r_3 \geq 0.5$ and $r_7 \geq 0.5$ **then**
          Update the MRs locations using case 4 of (7)
        end if
        Condition at Top layer
      else if ($|E| < 0.5$ and $\mathrm{r} < 0.5$) **then**
        Condition at Bottom and Middle layers
        if $r_3 < 0.5$ and $r_7 < 0.5$ **then**
          Update the MRs locations using case 11 or 21 of (8)
        else if $r_3 < 0.5$ and $r_7 \geq 0.5$ **then**
          Update the MRs locations using case 12 or 22 of (8)
        else if $r_3 \geq 0.5$ and $r_7 < 0.5$ **then**
          Update the MRs locations using case 13 or 23 of (8)
        else if $r_3 \geq 0.5$ and $r_7 \geq 0.5$ **then**
          Update the MRs locations using case 14 or 24 of (8)
        end if
        Condition at Top layer
      else if ($|E| \geq 0.5$ & $\mathrm{r} \geq 0.5$) **then**
        Condition at Bottom and Middle layers
        if $r_3 < 0.5$ and $r_7 < 0.5$ **then**
          Update the MRs locations using case 1 of (12)
        else if $r_3 < 0.5$ and $r_7 \geq 0.5$ **then**
          Update the MRs locations using case 2 of (12)
        else if $r_3 \geq 0.5$ and $r_7 < 0.5$ **then**
          Update the MRs locations using case 3 of (12)
        else if $r_3 \geq 0.5$ and $r_7 \geq 0.5$ **then**
          Update the MRs locations using case 4 of (12)
        end if
        Condition at Top layer
      else if ($|E| \geq 0.5$ & $\mathrm{r} < 0.5$) **then**
        Condition at Bottom and Middle layers
        if $r_3 < 0.5$ and $r_7 < 0.5$ **then**

The configuration parameters of HHO, SCA, GWO, PSO, EO, MFO and TSO are set to the same values based on original works recommendation. Table 2 presents the parameters' values in this configuration setup. In addition, the WMN charachterstic parameters are outlined in Table 3.

Algorithm 1 (*continued*)

Update the MRs locations using case 11 or 21 of (13)
else if $r_3 < 0.5$ and $r_7 \geq 0.5$ **then**
Update the MRs locations using case 12 or 22 of (13)
else if $r_3 \geq 0.5$ and $r_7 < 0.5$ **then**
Update the MRs locations using case 13 or 23 of (13)
else if $r_3 \geq 0.5$ and $r_7 \geq 0.5$ **then**
Update the MRs locations using case 14 or 24 of (13)
end if
end if
end if
end for
$t = t+1$
end while
Return Y_{prey} representing the optimum WMN topology with full routers connectivity and maximum clients coverage

3.4. Fitness function for optimizing WMN

The main objective of the novel TTHHO algorithm is to optimize the performance of the WMN by maximizing both network coverage and connectivity while utilizing less routers to reduce network congestion. The coverage metric, denoted as $\alpha(G)$ and expressed in (15), quantifies the extent to which the network provides coverage to clients. Additionally, the connectivity factor, denoted by $\theta(G)$ and represented by (16), is considered to measure the interconnectivity between routers in the network. To create the fitness function, a weighted sum approach is employed, transforming the multi-objective problem into a single-objective one by summing the individual goals with user-defined weights. Consequently, the fitness function, denoted as F_t and formulated in (17), integrates both client coverage and network connectivity metrics, guiding the optimization process towards achieving an efficient and well-balanced WMN configuration.

$$\alpha(G) = \sum_{i=0}^{m} \delta_i \tag{15}$$

$$\theta(G) = \max_{i \in \{1,\ldots,h\}} |G_i| \tag{16}$$

$$F_t = (1-\zeta) \cdot \left(1 - \frac{\alpha(G)}{m}\right) + \zeta \cdot \left(1 - \frac{\theta(G)}{n}\right) \tag{17}$$

where m represents the number of clients, n represents the number of routers, $\alpha(G)$ and $\theta(G)$ denotes the network coverage and connectivity. δ_i and G_i represent the number of covered clients and the size of sub-graph, respectively. The weighting coefficient ζ takes values between 0 and 1, representing the relative importance assigned to each objective's rank. To ensure normalization, the denominator should be used in each part of the equation, allowing for fair comparison of different objectives. The goal is to minimize the cost function, and ideally, it should approach the global minimum, which is zero. This indicates the optimal configuration of the WMN that maximizes coverage and connectivity.

The proposed approach in this work also addresses the optimal placement of the sink node in WMN by introducing a fitness function that evaluates the residual energy of neighboring nodes. The primary goal is to identify areas with higher residual energy within the network's neighborhood to strategically position the sink node. The fitness function used in this approach is based on evaluating the residual energy of neighbor nodes, which is a crucial factor in determining their remaining energy resources. By considering the residual energy, the fitness function identifies candidate locations for the sink node, where the neighboring nodes exhibit higher energy levels. Placing the sink node in such areas contributes to higher network longevity, as it ensures that the sink node can be efficiently replaced by a neighboring node in case it depletes its energy reserves.

The proposed objective function, represented by (18), plays a pivotal role in optimizing the sink node's placement. By employing this objective function, the algorithm can effectively identify the node with the highest residual energy among the neighbors, facilitating the selection of the most suitable location for the sink node. This decision-making process ensures that the sink node is strategically positioned in areas where it can be replaced by nodes with sufficient energy, contributing to the overall network's longevity and robustness.

$$f_t(n) = \frac{1}{\varrho_1 \sum_{t=1}^{X_{nbr}} E_{nbr}(t) + E_n + \varrho_2 X_{nbr} + \varrho_3 d_n} \tag{18}$$

where X_{nbr} represents the number of neighbor mesh routers of the sink node, E_{nbr} denotes the energy of these mesh routers, E_n is the candidate sink node n residual energy, d_n represents the position of the n node with respect to deployment area center and the parameters ϱ_1, ϱ_2, and ϱ_3 are random variables ranging from 0 to 1.

This research also tackles congestion reduction by minimizing network overlap while ensuring optimal levels of connectivity and coverage. The approach involves the application of a specific formula, designated as (19). This formula is instrumental in achieving a balance between reducing network congestion and maintaining effective network coverage and connectivity, thereby optimizing network performance.

$$\begin{aligned}
&\check{C} = \mathbb{R} - \sum_{i=1}^{\mathbb{R}} \left(\gamma_i + \varnothing_i\right), \quad \gamma_i \neq \varnothing_i \\
&\gamma = \begin{cases} 1 & d \geq x \\ 0 & d > x \end{cases} \\
&\varnothing = \begin{cases} 1 & \text{if the mesh router has no task} \\ 0 & \text{otherwise} \end{cases} \\
&x = \sqrt{\left(r_{x1} - r_{x2}\right)^2 + \left(r_{y1} - r_{y2}\right)^2}
\end{aligned} \tag{19}$$

where $\check{C}$ denotes the number of congested routers, $\mathbb{R}$ represents the total count of mesh routers, d is the user-defined desired distance, γ signifies the number of overlaying routers, $\varnothing$ refers to routers not assigned any task, and x denotes the Euclidean distance between any pair of routers.

4. Results and discussion

4.1. Validation of the proposed TTHHO

The proposed TTHHO algorithm's effectiveness is extensively evaluated through multiple assessment and a comparison with seven widely recognized algorithms. A set of 33 diverse benchmarking functions is employed to assess the robustness and practicality of TTHHO. The results of these equations are initially depicted through plots, then by thorough convergence studies and statistical analyses. The test Friedman ranking is then applied to assess the rank of the proposed TTHHO in comparison to the competing approaches. Furthermore, the TTHHO algorithm is employed to optimize the performance metrics of WMN, aiming to enhance its overall performance and efficiency.

4.1.1. Benchmark functions

Various benchmark functions are carefully selected for validation, taking into account factors such as multiple local minima, boundaries, dimensions, and constraints. Table 4 outlines these benchmark functions which are categorized into multi-modal, uni-modal, and hybrid systems to facilitate their classification. The algorithm's exploitation accuracy is assessed using uni-modal functions (F1 to F6) which possess a single global optima. Additionally, multi-modal functions are employed to assess the ability of the proposed approach in avoiding local optimal entrapment and reaching the final global optima, thereby demonstrating its exploration capability. Multi-modal functions (F7 to F10) with variable dimensions and multi-modal functions (F11 to F18) with non-varying dimensions are employed to assess the algorithm's stability under diverse conditions. Furthermore, hybrid functions (F19 to F33) assess the TTHHO proficiency in identifying space search local and global minima, as well as determining the next position movement in the search space. By utilizing this diverse set of benchmark functions, a comprehensive assessment of the performance and effectiveness of the TTHHO algorithm is achieved.

Moreover, Fig. 3 displays surface plots of the benchmark functions, showcasing a diverse array of shapes that correspond to their unique characteristics. These shapes include bowel, cone, plate, valley, and egg holder-shaped functions, each with distinct features and exhibiting single and multiple dimensions with single and multiple local minima value. Throughout the simulation, the maximum number of iterations and the swarms remain unchanged at 500 and 30, respectively. Other key optimization constants are set as follows: max $= 1.0$, min $= 0.2$, $\alpha = 5$, $\mu = 0.499$, and $\epsilon = 2.2204 \times 10^{-16}$. These well-defined settings ensure consistent and reliable evaluations of the proposed TTHHO algorithm across various benchmark functions with different complexities and characteristics.

4.1.2. Numerical analysis benchmark functions

This section involves a numerical comparison of the proposed TTHHO algorithm with other established optimization approaches, including TSO, PSO, GWO, SCA, EO, MFO, and HHO. Table 5 provides an example of the statistical parameters, comprising the mean, worst, best, and standard deviation of all competing algorithms, including F1, F16, F33. Similar comparisons are illustrated for the remaining benchmark functions in Fig. 4, focusing on the ranks obtained by each algorithm. These ranks are determined using the Friedman test, where the algorithms are ordered based on their mean values. A rank 1 signifies an algorithm that approaches the global minimum more closely, while a rank 8 indicates an algorithm that is farther from the global minima.

The evaluation of algorithm performance centers around measuring the proximity of the data statistics to the global minima for the tested benchmarking functions. Among all the algorithms, the proposed TTHHO consistently exhibits the lowest performance indices. Notably, the smallest mean value indicates TTHHO's capacity to discover better optima with smaller fitness functions, whereas the lower standard deviation (Stdv) reflects its best convergence reliability and stability. Consequently, TTHHO successfully avoids local optima, making it a robust optimization approach.

The rank values depicted in Fig. 4 further support this claim, showing that the proposed TTHHO algorithm outperforms other algorithms, particularly in various unimodal functions. HHO and TSO emerge as close competitors, closely approaching global optima in most statistical comparisons. Conversely, PSO demonstrates poor performance when evaluating statistical parameters, while GWO exhibits an unstable response, performing well in some functions but showing degradation in others. These results highlight the

Table 4
The mathematical model of the benchmark functions.

Function	Boundaries	Formula
F1	[-100,100]	$F(\mathbf{x}) = \sum_{i=1}^{n} x_i^2$
F2	[-10,10]	$F(\mathbf{x}) = \sum_{i=0}^{n} \lvert x_i \rvert + \prod_{i=0}^{n} \lvert x_i \rvert$
F3	[-100,100]	$F(\mathbf{x}) = \sum_{i=1}^{d} \left(\sum_{j=1}^{i} x_j \right)^2$
F4	[-30,30]	$F(\mathbf{x}) = \sum_{i=1}^{n-1} \left[100 \left(x_i^2 - x_{i+1} \right)^2 + \left(1 - x_i \right)^2 \right]$
F5	[-100,100]	$F(\mathbf{x}) = \sum_{i=1}^{n} \left(\left[x_i + 0.5 \right] \right)^2$
F6	[-128,128]	$F(\mathbf{x}) = \sum_{i=0}^{n} i x_i^4 + \mathrm{random}(0,1)$
F7	[-500,500]	$F(\mathbf{x}) = \sum_{i=1}^{n} \left(-x_i \sin \left(\sqrt{\lvert x_i \rvert} \right) \right)$
F8	[-32,32]	$F(\mathbf{x}) = -20 \exp \left(-0.2 \sqrt{\frac{1}{n} \sum_{i=1}^{n} x_i^2} \right) - \exp \left(\frac{1}{n} \sum_{i=1}^{n} \cos \left(2\pi x_i \right) \right) + 20 + e$
F9	[-50,50]	$F(\mathbf{x}) = \frac{\pi}{n} \left\{ 10 \sin \left(\pi y_1 \right) \right\} + \sum_{i=1}^{n-1} \left(y_i - 1 \right)^2 [1 + 10 \sin^2 \left(\pi y_{i+1} \right) + \sum_{i=1}^{n} u \left(x_i, 10, 100, 4 \right) \Bigg]$, where, $y_i = 1 + \frac{x_i + 1}{4}, u \left(x_i, a, k, m \right) \begin{cases} K \left(x_i - a \right)^m & \text{if } x_i > a \\ 0 & -a \leq x_i \geq a \\ K \left(-x_i - a \right)^m & -a \leq x_i \end{cases}$
F10	[-50,50]	$F(\mathbf{x}) = 0.1 \Bigg(\sin^2 \left(3\pi x_1 \right) + \sum_{i=1}^{n} \left(x_i - 1 \right)^2 \left[1 + \sin^2 \left(3\pi x_i + \quad 1 \right) \ \right] + \left(x_n - 1 \right)^2 1 + \sin^2 \left(2\pi x_n \right) \Bigg) + \sum_{i=1}^{n} u \left(x_i, 5, 100, 4 \right)$
F11	[-65,65]	$F(\mathbf{x}) = \left(\frac{1}{500} + \sum_{j=1}^{25} \frac{1}{j + \sum_{i=1}^{2}} \left(x_i - a_{ij} \right) \right)^{-1}$
F12	[-5,5]	$F(\mathbf{x}) = \sum_{i=1}^{11} \left[a_i - \frac{x_1 \left(b_i^2 + b_i x_2 \right)}{b_i^2 + b_i x_3 + x_4} \right]^2$
F13	[-5,5]	$F(\mathbf{x}) = 4x_1^2 - 2.1x_1^4 + \frac{1}{3} x_1^6 + x_1 x_2 - 4x_2^2 + 4x_2^4$
F14	[-5,5]	$F(\mathbf{x}) = \left(x_2 - \frac{5.1}{4\pi^2} x_1^2 + \frac{5}{\pi} x_1 - 6 \right)^2 + 10 \left(1 - \frac{1}{8\pi} \right) \cos x_1 + 10$
F15	[-4,5]	$f(\mathbf{x}) = \sum_{i=1}^{d/4} (x_{4i-3} + 10x_{4i-2})^2 + 5(x_{4i-1} - x_{4i})^2 + \quad (x_{4i-2} - 2x_{4i-1})^4 + 10 \left(x_{4i-3} - x_{4i} \right)^4$
F16	[-1,2]	$F(\mathbf{x}) = -\sum_{i=1}^{4} c_i \exp \left(-\sum_{i=1}^{3} a_{ij} \left(x_j - p_{ij} \right)^2 \right)$
F17	[0,1]	$F(\mathbf{x}) = -\sum_{i=1}^{4} c_i \exp \left(-\sum_{i=1}^{6} a_{ij} \left(x_j - p_{ij} \right)^2 \right)$
F18	[0,1]	$F(\mathbf{x}) = -\sum_{i=1}^{5} \left[\left(X - a_i \right) \left(X - a_i \right)^T + c_i \right]^{-1}$
F19	[-512,512]	$F(\mathbf{x}) = -(x_2 + 47) \sin(\sqrt{\lvert x_2 + \frac{x_1}{2} + 47 \rvert}) - \quad x_1 \sin(\sqrt{\lvert x_1 - (x_2 + 47) \rvert})$
F20	[-10,10]	$F(\mathbf{x}) = -\left\lvert \sin \left(x_1 \right) \cos \left(x_2 \right) \exp \left(\left\lvert 1 - \frac{\sqrt{x_1^2 + x_2^2}}{\pi} \right\rvert \right) \right\rvert$
F21	[-5.12,5.12]	$F(\mathbf{x}) = \left(\sum_{i=1}^{5} i \cos \left((i+1) x_1 + i \right) \right) \left(\sum_{i=1}^{5} i \cos \left((i+1) x_2 + i \right) \right)$
F22	[1.5,4]	$F(\mathbf{x}) = \sin \left(x_1 + x_2 \right) + \left(x_1 - x_2 \right)^2 - 1.5x_1 + 2.5x_2 + 1$
F23	[3,3]	$F(\mathbf{x}) = \left(4 - 2.1x_1^2 + \frac{x_1^4}{3} \right) x_1^2 + x_1 x_2 + \left(-4 + 4x_2^2 \right) x_2^2$
F24	[-100,100]	$F(\mathbf{x}) = -\cos \left(x_1 \right) \cos \left(x_2 \right) \exp \left(-\left(x_1 - \pi \right)^2 - \left(x_2 - \pi \right)^2 \right)$
F25	[-5,10]	$F(\mathbf{x}) = a \left(x_2 - b x_1^2 + c x_1 - r \right)^2 + s(1 - t) \cos \left(x_1 \right) + s$
F26	[-2,2]	$F(\mathbf{x}) = [1 + (x_1 + x_2 + 1)^2 (19 - 14x_1 + 3x_1^2 - 14x_2 + 6x_1 x_2 + 3x_2^2)] \times [30 + (2x_1 - 3x_2)^2 (18 - 32x_1 + 12x_1^2 + 48x_2 - 36x_1 x_2 + 27x_2^2)]$
F27	[-5,5]	$F(\mathbf{x}) = \frac{1}{2} \sum_{i=1}^{d} \left(x_i^4 - 16x_i^2 + 5x_i \right)$

Table 4 (*continued*)

Function	Boundaries	Formula
F28	[-10,10]	$F(\mathbf{x}) = \sin^2(\pi w_1) + \sum_{i=1}^{d-1}(w_i - 1)^2[1 + 10\sin^2(\pi w_i + 1)] + (w_d - 1)^2[1 + \sin^2(2\pi w_d)]$, where , $w_i = 1 + \frac{x_i - 1}{4}$, for all $i = 1, \ldots, d$
F29	[-10,10]	$F(\mathbf{x}) = 100\left(x_1^2 - x_2\right)^2 + \left(x_1 - 1\right)^2 + \left(x_3 - 1\right)^2 + 90\left(x_3^2 - x_4\right)^2 + 10.1\left(\left(x_2 - 1\right)^2 + \left(x_4 - 1\right)^2\right) + 19.8\left(x_2 - 1\right)\left(x_4 - 1\right)$
F30	[0,1]	$F(\mathbf{x}) = -\sum_{i=1}^{4}\alpha_i \exp\left(-\sum_{j=1}^{3} A_{ij}\left(x_j - P_{ij}\right)^2\right)$, where, $\alpha = (1.0, 1.2, 3.0, 3.2)^T$ $\mathbf{A} = \begin{pmatrix} 3.0 & 10 & 30 \\ 0.1 & 10 & 35 \\ 3.0 & 10 & 30 \\ 0.1 & 10 & 35 \end{pmatrix} \mathbf{P} = 10^{-4}\begin{pmatrix} 3689 & 1170 & 2673 \\ 4699 & 4387 & 7470 \\ 1091 & 8732 & 5547 \\ 381 & 5743 & 8828 \end{pmatrix}$
F31	[0,10]	$F(\mathbf{x}) = -\sum_{i=1}^{m}\left(\sum_{j=1}^{4}\left(x_j - C_{ji}\right)^2 + \beta_i\right)^{-1}$, where, $m = 10; \beta = \frac{1}{10}(1, 2, 2, 4, 4, 6, 3, 7, 5, 5)^T$ $\mathbf{C} = \begin{pmatrix} 4.0 & 1.0 & 8.0 & 6.0 & 3.0 & 2.0 & 5.0 & 8.0 & 6.0 & 7.0 \\ 4.0 & 1.0 & 8.0 & 6.0 & 7.0 & 9.0 & 3.0 & 1.0 & 2.0 & 3.6 \\ 4.0 & 1.0 & 8.0 & 6.0 & 3.0 & 2.0 & 5.0 & 8.0 & 6.0 & 7.0 \\ 4.0 & 1.0 & 8.0 & 6.0 & 7.0 & 9.0 & 3.0 & 1.0 & 2.0 & 3.6 \end{pmatrix}$
F32		$F(\mathbf{x}) = -\sum_{i=1}^{4}\alpha_i \exp\left(-\sum_{j=1}^{6} A_{ij}\left(x_j - P_{ij}\right)^2\right)$, where, $\alpha = (1.0, 1.2, 3.0, 3.2)^T$ $\mathbf{A} = \begin{pmatrix} 10 & 3 & 17 & 3.50 & 1.7 & 8 \\ 0.05 & 10 & 17 & 0.1 & 8 & 14 \\ 3 & 3.5 & 1.7 & 10 & 17 & 8 \\ 17 & 8 & 0.05 & 10 & 0.1 & 14 \end{pmatrix}, \mathbf{P} = 10^{-4}\begin{pmatrix} 1312 & 1696 & 5569 & 124 & 8283 & 5886 \\ 2329 & 4135 & 8307 & 3736 & 1004 & 9991 \\ 2348 & 1451 & 3522 & 2883 & 3047 & 6650 \\ 4047 & 8828 & 8732 & 5743 & 1091 & 381 \end{pmatrix}$
F33	[0,π]	$F(\mathbf{x}) = -\sum_{i=1}^{d}\sin\left(x_i\right)\sin^{2m}\left(\frac{ix_i^2}{\pi}\right)$

Table 5
TTHHO statistical and rank results compared to the competing algorithms.

Func.	G_m	STAT	HHO	SCA	GWO	PSO	MFO	EO	TSO	TTHHO
F1	0	**Mean**	4.18E-99	9.66E-74	1.53E-27	4.19E+04	3.01E+03	1.53E-41	2.25E-118	6.58E-134
		Best	4.44E-111	5.21E-87	2.24E-28	3.40E+04	2.73E+00	4.22E-42	4.78E-141	4.35E-142
		Worst	5.78E-99	5.57E-71	1.64E-27	5.01E+04	1.00E+04	6.59E-41	1.35E-99	1.39E-128
		Stdv	1.85E-99	1.75E-71	4.48E-28	4.94E+03	4.21E+03	1.91E-41	4.24E-100	4.38E-129
		Rank	3	4	6	8	7	5	2	1
F16	-3.86	**Mean**	-3.86E+00	-3.86E+00	-7.33E-01	-3.26E+00	-3.86E+00	-3.86E+00	-3.79E+00	-3.85E+00
		Best	-3.86E+00	-3.86E+00	-2.81E+00	-3.61E+00	-3.86E+00	-3.86E+00	-3.86E+00	-3.86E+00
		Worst	-3.85E+00	-3.85E+00	-9.54E-02	-2.66E+00	-3.86E+00	-3.86E+00	-3.61E+00	-3.84E+00
		Stdv	2.92E-03	3.17E-03	9.54E-01	3.47E-01	9.36E-16	7.69E-16	8.43E-02	8.53E-03
		Rank	1	1	8	7	1	1	6	1
F33	-9.6601	**Mean**	-5.76E+00	-9.82E-01	-8.02E+00	-2.96E+00	-7.86E+00	-8.60E+00	-5.69E+00	-5.83E+00
		Best	-6.87E+00	-2.12E+00	-8.84E+00	-4.09E+00	-8.60E+00	-9.26E+00	-6.89E+00	-6.86E+00
		Worst	-5.09E+00	-2.86E-03	-7.10E+00	-2.36E+00	-6.78E+00	-7.29E+00	-4.91E+00	-4.48E+00
		Stdv	5.62E-01	6.81E-01	6.40E-01	5.72E-01	7.17E-01	6.43E-01	6.66E-01	7.28E-01
		Rank	5	8	2	7	3	1	6	4
Mean of rank			2.2121	4.3030	4.8182	7.0303	3.6061	3.2121	2.9697	**1.7879**
Final rank			2	6	7	8	5	4	3	**1**

enhancement of exploration accuracy using TTHHO. In the analysis of different multimodal functions, TTHHO displays extraordinary exploration capabilities, effortlessly transitioning between local minima values while avoiding being trapped. Likewise, the TTHHO excels in most hybrid functions, showcasing its superior capability to identify optimal values. Many functions with non-zero or numerous local minima have their optimal solutions discovered in the early stage of HHO or TTHHO's search, underscoring the effectiveness of the proposed approach in handling complex optimization landscapes.

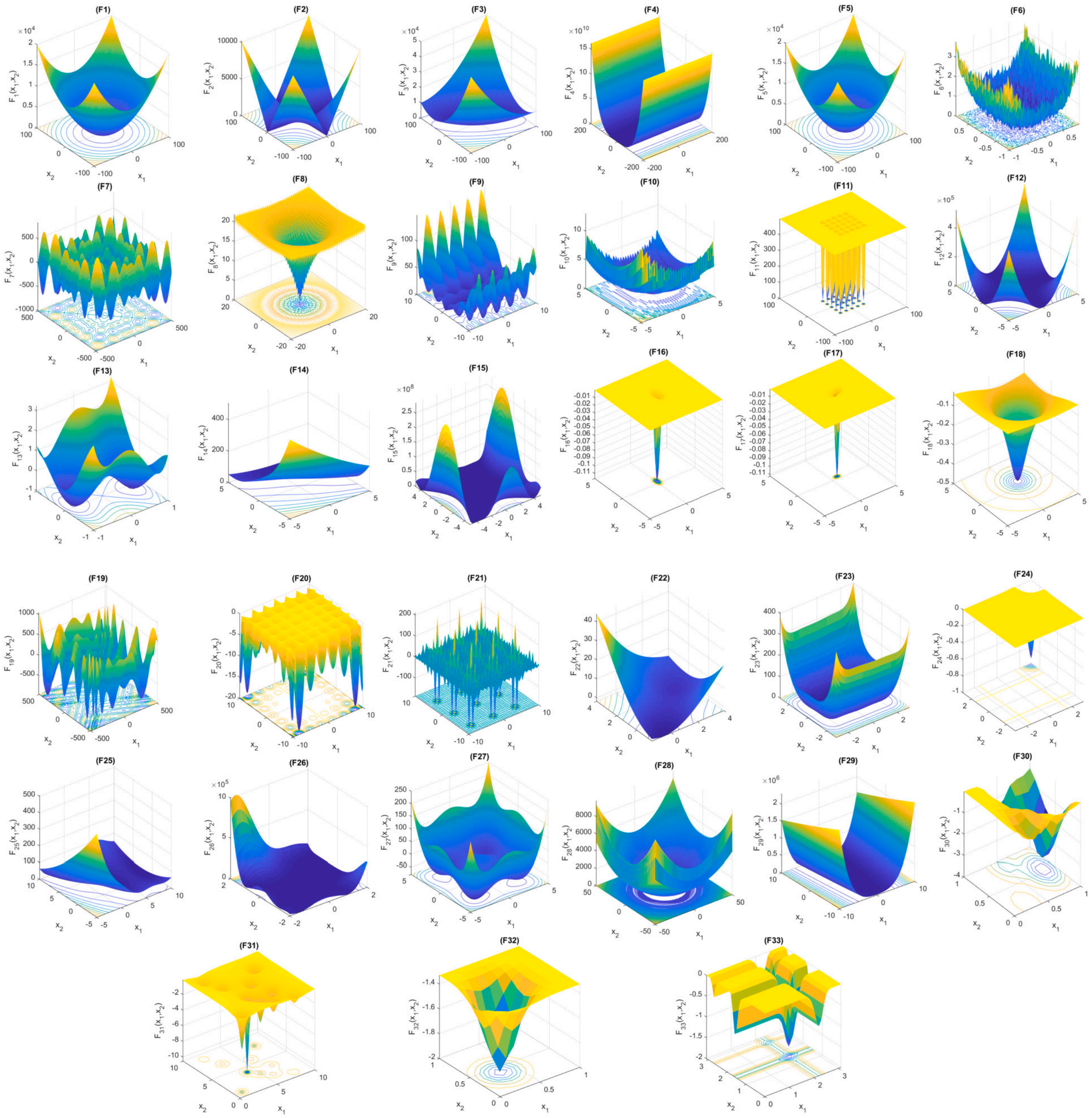

Fig. 3. The graphical depiction of the benchmark functions.

The proposed TTHHO algorithm attained an impressive minimum mean value of 1.7879, showcasing its superior performance and securing the top rank in the comparison. Following TTHHO, the rankings of the other algorithms, in descending order, are HHO, TSO, EO, MFO, SCA, GWO, and PSO. This clear difference in mean values highlights the significant enhancement in search capability and consistency achieved by the proposed hybrid method, demonstrating its effectiveness over existing techniques.

4.1.3. Convergence analysis of the benchmark functions

The benchmark functions underwent rigorous testing with 300 iterations each to analyze their convergence. In this context, “convergence” refers to the point at which an algorithm locates the minimal fitness value within the scheduled maximum iterations. Fig. 5 displays the convergence plots of the benchmark functions, highlighting the performance of various algorithms, including the proposed TTHHO.

In the category of unimodal benchmark functions, the proposed TTHHO demonstrated a broad search strategy, leading to the exploration of diverse solutions and necessitating further iterations. Despite this behavior, TTHHO showcased a remarkable enhance-

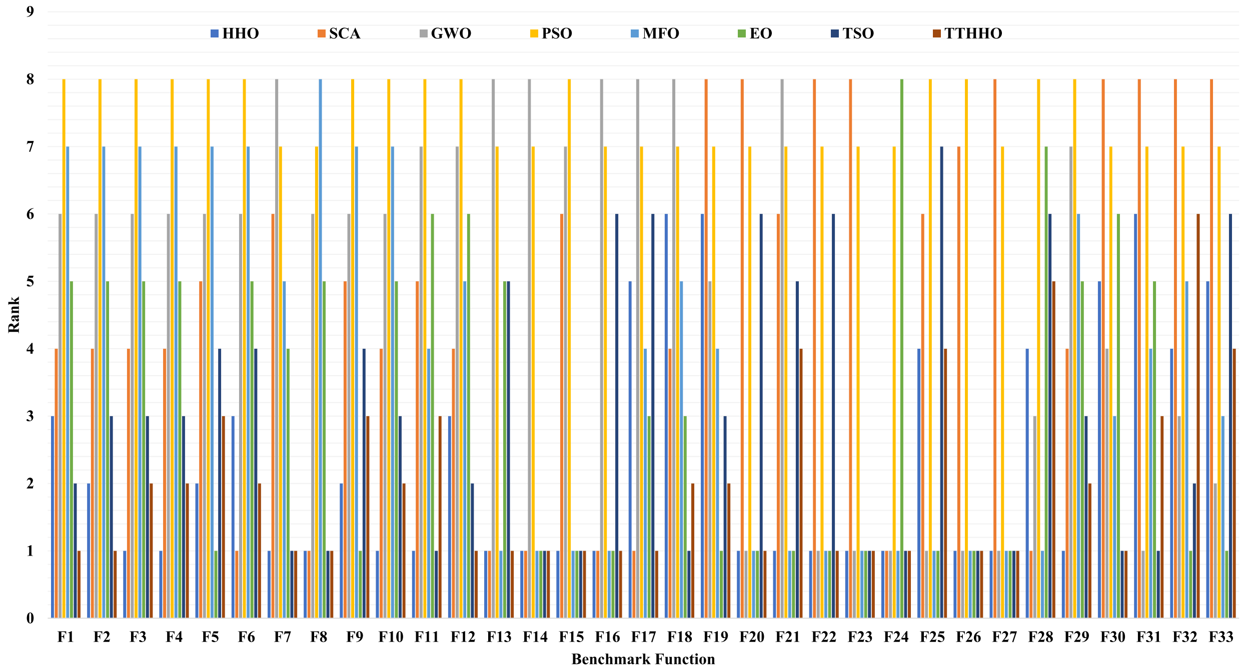

Fig. 4. The rank value of TTHHO vs other algorithms using 33-benchmark functions.

ment in approaching the global minima. The Friedman ranking method confirmed this outstanding performance by awarding the proposed TTHHO the first rank, attributing to its best mean in speculating the global minima. Notably, the second closest competitors to TTHHO, namely HHO and SCA, also performed well in the Friedman ranking. On the other hand, GWO displayed relatively limited effectiveness in dealing with unimodal functions, while PSO exhibited the poorest performance, displaying a substantial gap between the obtained value and the desired global minimum.

The findings emphasize the proficiency of the proposed TTHHO algorithm in tackling unimodal benchmark functions by striking a balance between exploration and exploitation to effectively converge towards the global minima. The visualization in Fig. 5 underscores the superiority of TTHHO and positions it as a leading choice for optimization tasks, showcasing its potential to surpass competing algorithms in challenging scenarios.

In summary, the analyses of convergence confirm the ranking Friedman test for the proposed TTHHO algorithm alongside the competing algorithms, resulting in the following ranking: TTHHO obtained the first rank, while HHO and TSO obtained the second and third positions in the overall performance assessment among the 33 benchmark functions. Conversely, GWO and PSO secured the seventh and eighth rankings, respectively.

4.2. WMN optimization analyses using the proposed TTHHO

The performance of the proposed TTHHO algorithm in optimizing the WMN is thoroughly analyzed by comparing it with seven well-known algorithms based on various metrics, including fitness value, convergence, connectivity and coverage, and residual energy. This section presents a comprehensive discussion of the findings obtained through the utilization of TTHHO for WMN optimization.

4.2.1. Convergence analysis of TTHHO for different WMN network sizes

The convergence Fig. 6 displays the TTHHO performance compared to different optimization algorithms for various network sizes. Each sub-figure corresponds to a specific network size ranging from 60 to 160 routers.

Upon analyzing the convergence figure, it becomes evident that the proposed TTHHO algorithm consistently outperforms the other algorithms in terms of convergence. For smaller network sizes, such as 60 routers in Fig. 6a and 80 routers as in Fig. 6b, TTHHO achieves a convergence value of 0.1733 and 0.0675, respectively. In contrast, the convergence values of the other algorithms range from 0.0712 to 0.32 for 80 routers. This suggests that TTHHO converges faster and more accurately to optimal or near-optimal solutions, making it a preferable choice for networks of modest size.

As the network size increases, the performance gap between TTHHO and the other algorithms widens. Figs. 6c, 6d and 6e represent the convergence curves for 100, 120 and 140 routers, respectively. Fig. 6f depicts the convergence curve for 160 routers network size where TTHHO attains an impressively low convergence value of 0.003125, while the other algorithms range from 0.003125 to 0.00625. This trend demonstrates the robustness of TTHHO in handling larger and more complex networks, where the search space becomes considerably more challenging to explore.

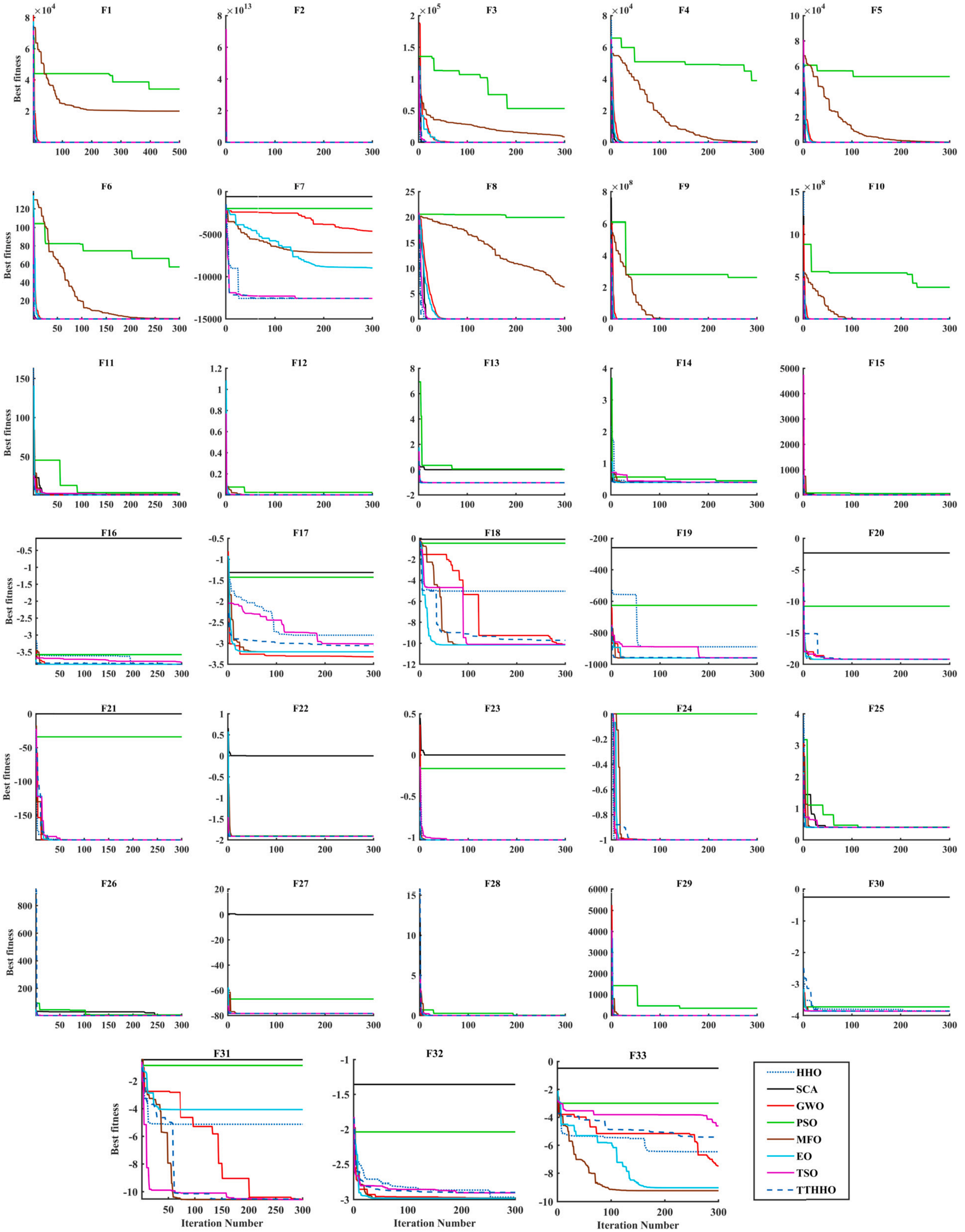

Fig. 5. Convergence curves of TTHHO vs other algorithms for the 33-benchmark functions.

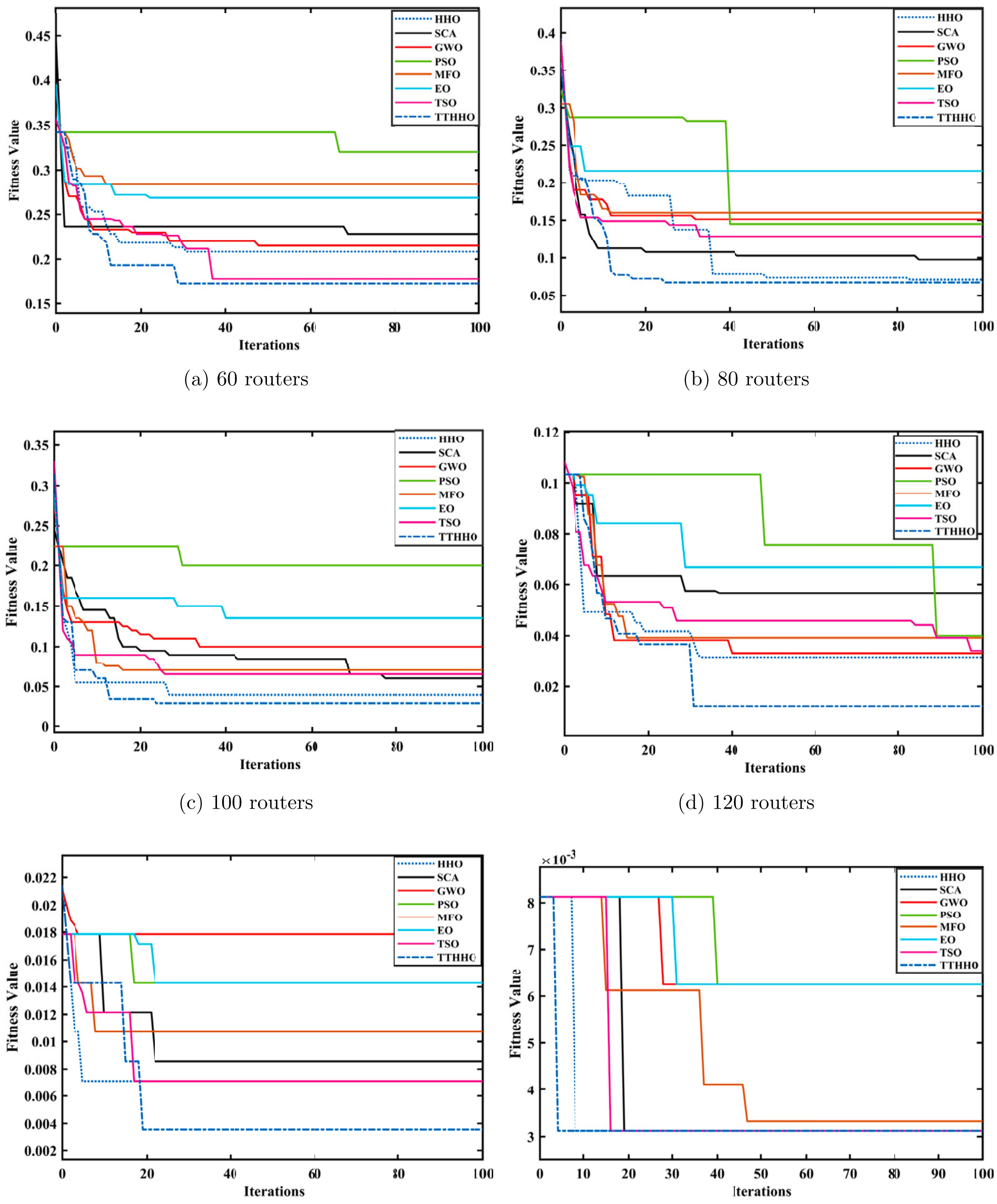

(a) 60 routers (b) 80 routers

(c) 100 routers (d) 120 routers

(e) 140 routers (f) 160 routers

Fig. 6. Convergence analysis for various network sizes.

Furthermore, the figure showcases TTHHO's exceptional ability to approach the global minimum effectively. The descending trend in convergence values with increasing network size suggests that TTHHO is adept at navigating complex search spaces and has a higher likelihood of converging to the global minimum. In contrast, other algorithms appear to struggle more with larger networks, as evidenced by their comparatively higher convergence values.

The figure's outcomes emphasize the significant advantages of employing the TTHHO algorithm for network optimization tasks. Its faster convergence and ability to achieve the global minimum make it a compelling choice, particularly for large-scale networks. TTHHO's unique combination of TSO, SCA and HHO enables it to explore the search space efficiently and refine solutions effectively, culminating in superior optimization performance across diverse network sizes.

4.2.2. Statistical analysis of TTHHO for different WMN network sizes

The effectiveness of the proposed TTHHO is statistically validated on different size of WMN ranging from 60 to 160 routers. Table 6 presents the fitness values average and variance which correspond to each network size.

The table outlines a comprehensive comparison of TTHHO with other algorithms concerning mean, best, worst, and standard deviation fitness values for 60 routers in a network. Among the algorithms, TTHHO exhibits the lowest mean fitness value of 0.2002, indicating its superior optimization performance. TTHHO also achieves an impressive best fitness value of 0.1733, surpassing all other algorithms in finding the most optimal solution. Moreover, TTHHO's worst fitness value of 0.25 is competitive and comparable to other high-performing algorithms. Notably, TTHHO displays the smallest standard deviation of 0.0013, which reflects its robustness and stability in consistently converging to quality solutions. Additionally, TTHHO exhibits the lowest average variance of fitness values at 0.000241, indicating its ability to consistently converge towards optimal solutions with minimal variation. This outstanding performance in terms of both mean fitness and variance emphasizes TTHHO's reliability and accuracy in optimization tasks. Overall, the findings unequivocally demonstrate that TTHHO outperforms the other algorithms, providing more accurate and reliable optimization results for the given network size.

Similarly, for 80 routers, TTHHO once again exhibits superior optimization performance with the lowest mean fitness value of 0.1044, outperforming all other algorithms. TTHHO also achieves the best fitness value of 0.0837, indicating its exceptional ability to find the most optimal solution. Additionally, TTHHO's worst fitness value of 0.16 is highly competitive, comparable to the top-performing algorithms. The small standard deviation of 0.0144 underscores TTHHO's stability and consistency in converging towards high-quality solutions with minimal fluctuation. Moreover, TTHHO demonstrates the lowest average variance of fitness values at 0.000201, signifying its remarkable ability to converge consistently towards optimal solutions while maintaining low variability. This exceptional performance in both mean fitness and variance further strengthens TTHHO's reliability and accuracy in tackling optimization challenges for network sizes with 80 routers. The results once again solidify TTHHO's dominance among the algorithms tested, highlighting its capacity to outperform competitors in terms of both convergence quality and stability. TTHHO's robustness and efficiency make it a compelling choice for optimizing networks with 80 routers, ensuring more accurate and dependable results for various real-world applications.

For 100 routers, TTHHO continues to demonstrate its exceptional optimization performance, obtaining the lowest mean fitness value of 0.0555 among all algorithms, emphasizing its superior ability to find optimal solutions. Similarly, TTHHO achieves the best fitness value of 0.03, outperforming other algorithms in reaching the most optimal solution. Additionally, TTHHO's worst fitness value of 0.11 remains highly competitive, showcasing its robustness across diverse scenarios. Furthermore, TTHHO maintains remarkable stability with the smallest standard deviation of 0.0154, signifying its consistency in achieving high-quality solutions. Moreover, TTHHO displays the lowest average variance of fitness values at 0.000222, underlining its reliability in consistently converging to optimal solutions with minimal variability. These impressive findings emphasize TTHHO's superiority as an optimization algorithm for networks with 100 routers, making it a compelling choice for achieving accurate and dependable results.

Consistently showcasing its superior optimization capabilities, TTHHO achieves the lowest mean fitness value of 0.0269, surpassing all other algorithms with 120 mesh routers. This emphasizes TTHHO's exceptional ability to find highly optimal solutions. TTHHO also secures the best fitness value of 0.0125, demonstrating its effectiveness in reaching the most optimal solution. Additionally, TTHHO's worst fitness value of 0.0425 remains competitive, signifying its robustness in diverse scenarios. Moreover, TTHHO exhibits remarkable stability with the smallest standard deviation of 0.0064, reaffirming its consistency in delivering high-quality solutions. Furthermore, TTHHO maintains the lowest average variance of fitness values at 0.000040, underlining its reliability in consistently converging towards optimal solutions with minimal variability.

For networks with 140 routers, the comparison table demonstrates the exceptional optimization capabilities of TTHHO in terms of both average fitness values and average variance of fitness values. TTHHO outperforms all other algorithms with the lowest mean fitness value of 0.0043, showcasing its ability to consistently find optimal solutions. Similarly, it achieves the best fitness value of 0.0036, indicating its effectiveness in reaching the most optimal solution. TTHHO's worst fitness value of 0.0107 remains highly competitive, highlighting its robustness across diverse network configurations. Furthermore, TTHHO maintains remarkable stability with the smallest standard deviation of 0.0024, confirming its consistency in delivering high-quality solutions. Impressively, TTHHO also displays low average variance of fitness values at 0.000006, affirming its reliability in consistently converging towards optimal solutions with minimal variability.

For 160 routers, the comparison table further establishes TTHHO as an outstanding optimization algorithm, showcasing its superiority in terms of average fitness values and average variance of fitness values. TTHHO achieves the lowest mean fitness value of 0.0032, outperforming all other algorithms and consistently converging towards optimal solutions. Similarly, TTHHO secures the best fitness value of 0.0031, emphasizing its remarkable ability to reach the most optimal solution. Additionally, TTHHO's worst fitness value of 0.0062 remains highly competitive, underscoring its robustness across various network configurations. Furthermore, TTHHO maintains remarkable stability with the smallest standard deviation of 0.00056, reaffirming its consistency in delivering high-quality solutions. Impressively, TTHHO also displays the lowest average variance of fitness values at 0.0000003, further confirming its reliability in consistently converging towards optimal solutions with virtually negligible variability. These compelling results reinforce TTHHO's position as a highly dependable optimization algorithm for networks with 160 routers, making it an ideal choice for achieving accurate and dependable results in real-world applications with large and complex networks.

In summary, the Table 6 outline statistical findings for network sizes ranging from 60 to 160 routers and demonstrates the exceptional optimization capabilities of TTHHO when compared to other algorithms. Across all network sizes, TTHHO consistently outperforms its counterparts in terms of mean fitness values, achieving lower values and converging faster to optimal or near-optimal solutions. TTHHO also excels in finding the global minimum, as evidenced by its progressively decreasing final convergence values with increasing network sizes. Moreover, TTHHO exhibits remarkable stability with smaller standard deviations and lower average variance of fitness values, making it a highly reliable and consistent optimization algorithm. These results emphasize TTHHO's

Table 6
WMN based Statistical Data of TTHHO vs other Algorithms.

60 Routers								
Algorithm	**Fitness average values**				**Fitness Variance average values**			
	Mean	**Best**	**Worst**	**Stdv**	**Mean**	**Best**	**Worst**	**Stdv**
HHO	0.211454	0.1583	0.2783	0.025295	0.000619	0.000712	0.000753	0.001718
SCA	0.225159	0.195	0.265	0.016838	0.000274	0.000304	0.000322	0.001637
GWO	0.213409	0.185	0.24	0.01603	0.000249	0.000275	0.00027	0.001472
PSO	0.286526	0.2083	0.3267	0.03132	0.000949	0.001149	0.000995	0.003012
MFO	0.255782	0.1967	0.2917	0.034005	0.001119	0.001237	0.001154	0.002688
EO	0.259899	0.2183	0.2833	0.016151	0.000252	0.000308	0.000269	0.002115
TSO	0.212999	0.1733	0.2583	0.022799	0.000503	0.000555	0.000564	0.001647
TTHHO	0.200172	0.1733	0.25	0.015787	0.000241	0.000265	0.000317	0.001309
80 Routers								
Algorithm	**Fitness average values**				**Fitness Variance average values**			
	Mean	**Best**	**Worst**	**Stdv**	**Mean**	**Best**	**Worst**	**Stdv**
HHO	0.123444	0.0875	0.17	0.023457	0.000533	0.000578	0.000594	0.000858
SCA	0.145047	0.1125	0.1888	0.020211	0.000395	0.000431	0.000451	0.000893
GWO	0.136427	0.085	0.17	0.021075	0.00043	0.000518	0.000461	0.000858
PSO	0.177159	0.1262	0.2175	0.024036	0.000559	0.000646	0.000606	0.001307
MFO	0.167113	0.1275	0.1962	0.018797	0.000342	0.000394	0.000366	0.001039
EO	0.199473	0.1687	0.2213	0.014746	0.00021	0.000241	0.000225	0.001282
TSO	0.131411	0.0875	0.1775	0.025646	0.000637	0.000704	0.000696	0.001002
TTHHO	0.104445	0.0837	0.16	0.01442	0.000201	0.000216	0.000295	0.000459
100 Routers								
Algorithm	**Fitness average values**				**Fitness Variance average values**			
	Mean	**Best**	**Worst**	**Stdv**	**Mean**	**Best**	**Worst**	**Stdv**
HHO	0.060359	0.025	0.115	0.024826	0.000577	0.000627	0.000654	0.000627
SCA	0.083827	0.03	0.155	0.028818	0.000778	0.000885	0.000914	0.000889
GWO	0.085668	0.045	0.125	0.020064	0.000377	0.000435	0.000419	0.000521
PSO	0.1444	0.07	0.2	0.034483	0.001113	0.001306	0.001194	0.001521
MFO	0.070866	0.035	0.11	0.019649	0.000361	0.000408	0.000402	0.000452
EO	0.122246	0.075	0.16	0.020971	0.000412	0.000487	0.000452	0.000744
TSO	0.074519	0.03	0.155	0.025795	0.000623	0.000696	0.000804	0.00071
TTHHO	0.055533	0.03	0.11	0.01541	0.000222	0.000245	0.000309	0.000277
120 Routers								
Algorithm	**Fitness average values**				**Fitness Variance average values**			
	Mean	**Best**	**Worst**	**Stdv**	**Mean**	**Best**	**Worst**	**Stdv**
HHO	0.027969	0.0175	0.0467	0.007131	4.92E-05	5.32E-05	5.92E-05	6.39E-05
SCA	0.035439	0.0167	0.0658	0.014148	0.000194	0.000208	0.000218	0.000212
GWO	0.038678	0.0208	0.0692	0.013191	0.000169	0.000181	0.000194	0.000192
PSO	0.058475	0.0258	0.1008	0.01818	0.00032	0.000359	0.000368	0.000378
MFO	0.04606	0.0175	0.0858	0.014321	0.000199	0.000228	0.000242	0.000234
EO	0.053345	0.0225	0.0783	0.013281	0.000171	0.000204	0.000187	0.000226
TSO	0.03367	0.0167	0.0608	0.009104	8.03E-05	9.06E-05	0.000101	0.000101
TTHHO	0.026915	0.0125	0.0425	0.006436	4.01E-05	4.73E-05	4.69E-05	5.42E-05

(*continued on next page*)

Table 6 (*continued*)

140 Routers								
Algorithm	**Fitness average values**				**Fitness Variance average values**			
	Mean	**Best**	**Worst**	**Stdv**	**Mean**	**Best**	**Worst**	**Stdv**
HHO	0.004395	0.0036	0.0107	0.0023	5.12E-06	5.16E-06	6.21E-06	5.31E-06
SCA	0.006784	0.0036	0.0143	0.003501	1.19E-05	1.24E-05	1.33E-05	1.24E-05
GWO	0.014295	0.0036	0.0336	0.009436	8.65E-05	9.22E-05	9.43E-05	8.82E-05
PSO	0.015925	0.007143	0.027857	0.005189	2.61E-05	2.89E-05	2.99E-05	3.02E-05
MFO	0.006172	0.003571	0.014286	0.003802	1.4E-05	1.44E-05	1.56E-05	1.43E-05
EO	0.021577	0.0107	0.0336	0.006308	3.85E-05	4.28E-05	4.24E-05	4.67E-05
TSO	0.004898	0.0036	0.0179	0.003524	1.2E-05	1.21E-05	1.67E-05	1.22E-05
TTHHO	0.004258	0.0036	0.0107	0.002449	5.81E-06	5.84E-06	6.94E-06	5.96E-06
160 Routers								
Algorithm	**Fitness average values**				**Fitness Variance average values**			
	Mean	**Best**	**Worst**	**Stdv**	**Mean**	**Best**	**Worst**	**Stdv**
HHO	0.003302	0.003125	0.008125	0.001042	1.05E-06	1.05E-06	1.75E-06	1.22E-06
SCA	0.003539	0.003125	0.008125	0.00134	1.74E-06	1.75E-06	2.35E-06	1.91E-06
GWO	0.007618	0.006312	0.01875	0.004357	1.84E-05	1.86E-05	2.36E-05	1.84E-05
PSO	0.007741	0.006312	0.01125	0.002709	7.11E-06	7.25E-06	8.19E-06	7.32E-06
MFO	0.003773	0.003254	0.00625	0.00078	5.88E-07	5.89E-07	8.54E-07	7.92E-07
EO	0.007891	0.006312	0.014375	0.002934	8.34E-06	9.24E-06	9.4E-06	9.3E-06
TSO	0.003792	0.003125	0.008125	0.00152	2.24E-06	2.26E-06	2.76E-06	2.43E-06
TTHHO	0.003198	0.003125	0.00625	0.000561	3.05E-07	3.05E-07	5.89E-07	5.27E-07

superiority and robustness across diverse network configurations, solidifying its position as an outstanding choice for achieving accurate and dependable results in real-world applications, especially for larger and more complex networks.

4.2.3. *Optimized WMN topology using TTHHO vs other algorithm*

Fig. 7 provides a comprehensive visual representation of the initial WMN and the optimized states achieved by the proposed TTHHO algorithm, as well as the competing algorithms. The initial WMN is depicted as a congested network with limited coverage, showing numerous congested paths and areas with weak or no wireless connectivity. This state exemplifies the challenges and inefficiencies faced by the network in its original configuration.

The comparison Fig. 7 showcases the remarkable performance of the proposed TTHHO algorithm against competing algorithms in WMN with 100 routers. Notably, the proposed TTHHO algorithm successfully optimizes the location of the sink node based on residual energy, ensuring increased network longevity. By strategically placing the sink node, TTHHO enhances energy efficiency, leading to extended network lifespans and improved overall network performance. This aspect sets TTHHO apart from other algorithms, as it demonstrates a deeper understanding of energy dynamics within the network, ultimately contributing to its superior optimization capabilities.

Furthermore, Fig. 7i highlights the outstanding achievements of the proposed TTHHO in terms of ensuring 100% coverage and 100% connectivity within the WMN. This can be observed by comparing it against initial topology in Fig. 7a and the algorithms. While the HHO algorithm, Fig. 7b, comes closest with 98% coverage, the proposed TTHHO surpasses all other competing algorithms by guaranteeing full coverage and connectivity, leaving no dead zones or isolated nodes. This achievement is of utmost significance in practical applications, as complete coverage and connectivity are critical for seamless communication and data transmission in WMNs. TTHHO's ability to achieve this feat showcases its versatility and adaptability in addressing real-world challenges effectively.

Indeed, the competing algorithms, EO and GWO as shown in Figs. 7g and 7d, achieved the lowest coverage rates of 93% and 94%, respectively, compared to the initial WMN state. These lower coverage rates indicate that EO and GWO were not as effective as other algorithms, including the proposed TTHHO, in ensuring that all areas within the network have reliable and consistent wireless connectivity. In addition, the TTHHO continues to show superior performance when compared against the optimized networks of the other algorithms such as SCA, PSO, MFO and TSO as shown in Figs. 7c, 7e, 7f and 7h, respectively.

Moreover, the proposed algorithm's effectiveness extends beyond coverage and connectivity improvements. The figure reveals that TTHHO excels in reducing network congestion at an unparalleled rate compared to other algorithms. Efficiently managing and minimizing congestion is crucial for enhancing network performance, reducing delays, and ensuring smooth data flow. TTHHO's competence in congestion reduction illustrates its ability to intelligently optimize the placement of routers and sink nodes, avoiding traffic bottlenecks and improving overall network throughput. The exceptional congestion reduction achieved by TTHHO further cements its position as an ideal and comprehensive solution for optimizing WMNs.

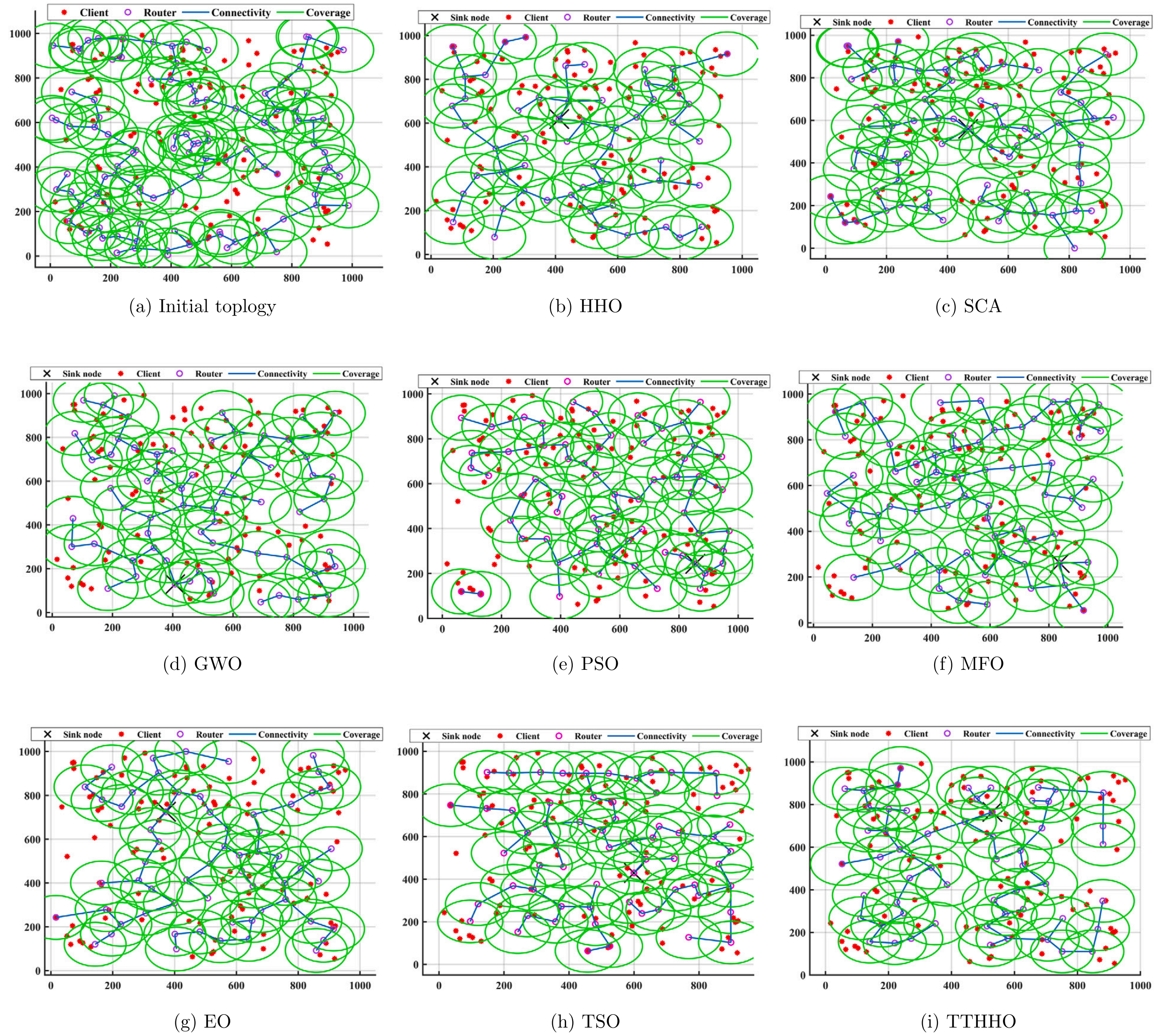

(a) Initial toplogy (b) HHO (c) SCA

(d) GWO (e) PSO (f) MFO

(g) EO (h) TSO (i) TTHHO

Fig. 7. Optimized WMN topology using TTHHO vs other algorithm.

In summary, the comparison Fig. 7 demonstrates the superiority of the proposed TTHHO algorithm in optimizing WMNs with 100 routers. Through its strategic sink node placement based on residual energy, TTHHO enhances network longevity and energy efficiency. Furthermore, it surpasses competing algorithms by ensuring 100% coverage and connectivity, eliminating dead zones, and isolated nodes. Additionally, TTHHO excels in reducing network congestion, leading to enhanced overall network performance. These exceptional attributes collectively establish TTHHO as a cutting-edge and highly effective algorithm for WMNs, offering significant advantages in terms of network longevity, coverage, connectivity, and congestion management.

4.2.4. Analysis of congestion reduction and coverage for various WMN sizes

Figs. 8 and 9 provide a comprehensive visualization of the congestion reduction and coverage for various WMN sizes, respectively. The figures clearly illustrate the consistent and superior performance of the proposed TTHHO algorithm compared to the other competing optimization techniques. In Fig. 8, TTHHO demonstrates TTHHO's remarkable effectiveness in reducing congestion within the WMN. By strategically placing the routers and sink node, TTHHO optimizes the network's traffic flow, leading to reduced congestion and improved data transmission efficiency.

For a network with 60 routers, TTHHO achieves an impressive congestion reduction percentage of 38.33%, outperforming most of the competing algorithms, such as HHO (28.33%), SCA (20%), GWO (28.33%), PSO (28.33%), MFO (13.33%), EO (43.33%), and TSO (11.67%). This significant reduction in congestion demonstrates TTHHO's ability to effectively optimize the network's structure, leading to enhanced data flow and reduced traffic bottlenecks.

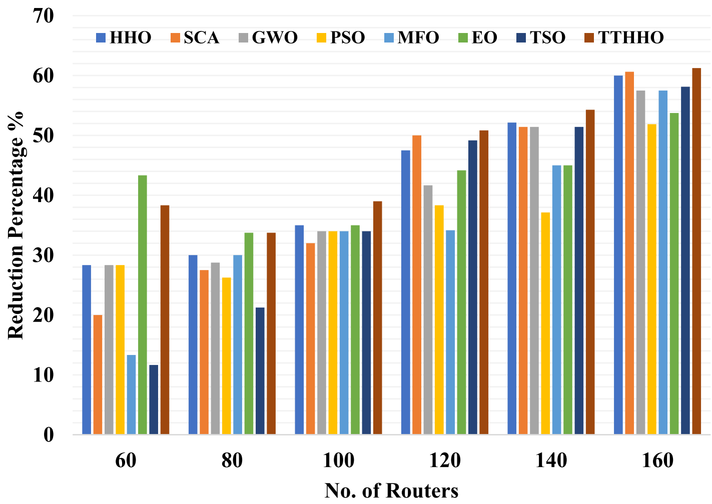

Fig. 8. WMN Congestion Reduction sizes using TTHHO vs other algorithm.

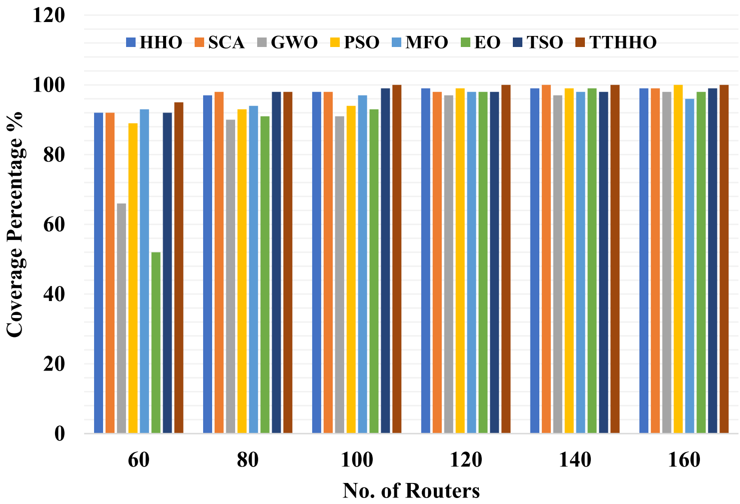

Fig. 9. WMN Client Coverage using TTHHO vs other algorithm.

As the network size further increases to 80, 100, 120, 140, and 160 routers, TTHHO maintains its lead in congestion reduction, showcasing percentages of 33.75%, 35%, 50.83%, 54.29%, and 61.25%, respectively. In comparison, the competing algorithms' performance fluctuates, with some achieving similar results to TTHHO in certain scenarios, but none consistently surpassing its congestion reduction capabilities across all network sizes. On the other hand, in the provided Fig. 9, one can observe the coverage percentage rates achieved by the TTHHO algorithm compared to other competing algorithms, namely HHO, SCA, GWO, PSO, MFO, EO, and TSO.

One notable observation is that despite achieving high congestion reduction, the TTHHO algorithm manages to provide significantly higher coverage to clients in the WMN, even when using fewer routers. Let's delve into the discussion of the coverage rates for different WMN sizes. For a WMN with 60 routers, TTHHO achieves an impressive coverage rate of 95%, outperforming all the other algorithms. This signifies that TTHHO effectively places the routers in strategic positions, ensuring that a vast majority of clients in the network receive reliable and stable connectivity.

As the WMN size increases to 80 and 100 routers, TTHHO maintains its dominance, consistently achieving the highest coverage rates of 98% and 100%, respectively. This remarkable performance demonstrates TTHHO's ability to adapt to different network sizes while ensuring extensive client coverage. Moreover, even when the number of routers increases to 120, 140, and 160, TTHHO continues to deliver outstanding results with coverage rates of 100% for all three cases. This illustrates the robustness and scalability of TTHHO, as it can effectively handle larger WMNs without compromising on coverage quality. In contrast, the other competing algorithms show varied and relatively lower coverage rates. Some algorithms, like GWO and EO, struggle to provide as extensive coverage as TTHHO, especially for larger network sizes.

Table 7
Residual Energy of TTHHO vs other algorithm for different WMN sizes.

Algorithm	No. Routers					
	60	80	100	120	140	160
HHO	9568.603	10009.43	11378.35	11538.07	12220.17	12879.32
SCA	8316.287	8524.386	10723.65	11267.39	11552.66	12151.34
GWO	9557.658	9831.855	10899.12	9831.477	10885.14	11035.66
PSO	8770.206	8982.251	10522.05	10993.48	11120.17	11641.83
MFO	9180.605	9527.857	10373.3	11248.98	11645.58	12031.21
EO	9283.487	9555.042	11354.27	11428.95	11830.56	12088.18
TSO	8837.745	8941.264	9851.015	11400.52	12848.39	13054.75
TTHHO	10097.99	10314.18	11579.68	11920.41	13308.7	13916.92

Overall, Figs. 8 and 9 demonstrate TTHHO's superiority in terms of coverage percentage rates compared to the competing algorithms. Despite achieving high congestion reduction and utilizing fewer routers, TTHHO excels in offering wider coverage to clients in the WMN, showcasing its effectiveness in optimizing the network structure for improved connectivity and client satisfaction. This compelling performance makes TTHHO an attractive choice for designing and optimizing WMNs, particularly in scenarios where maximizing coverage is a priority. Overall, the findings underscore the robustness and versatility of TTHHO, positioning it as a leading candidate for addressing the challenges of WMN design and operation, and contributing to seamless communication and enhanced network performance.

4.2.5. Residual energy analysis of the optimized WMN

Table 7 presents the residual energy values for different WMN sizes ranging from 60 to 160 routers, obtained using various optimization techniques, including HHO, SCA, GWO, PSO, MFO, EO, TSO, and the proposed TTHHO.

The residual energy represents the sum of energies within the cluster of the sink node, where the sink node's placement is optimized by each algorithm. The proposed TTHHO consistently demonstrates superior performance in obtaining higher residual energy compared to other competing algorithms. The higher residual energy obtained by TTHHO signifies more energy-efficient network configurations, as it reflects the better utilization of energy resources within the network.

Across all WMN sizes, TTHHO consistently outperforms other algorithms, such as HHO, SCA, GWO, PSO, MFO, EO, and TSO, in terms of residual energy. This consistent performance of TTHHO is noteworthy, as it indicates that the proposed algorithm excels in finding optimized sink node placements, leading to clusters with higher energy levels and improved network longevity. For instance, with 60 routers, TTHHO obtains a significantly higher residual energy of 10097.99 compared to the competing algorithms, where the highest residual energy achieved by HHO is 9568.6. This substantial difference indicates that TTHHO excels in clustering routers around the sink node in a way that preserves more energy resources.

Similarly, with 80 routers, TTHHO continues to outperform other algorithms, obtaining a residual energy of 10314.18. In contrast, the highest residual energy achieved by HHO is 10009.43. Again, this demonstrates TTHHO's superior ability to find optimal sink node placements, resulting in clusters with higher energy levels. The trend persists as the WMN size increases to 100 routers, where TTHHO achieves a remarkable residual energy value of 11579.68, surpassing the other algorithms, such as EO, which achieves 11354.27. This indicates that TTHHO optimizes the network structure effectively, leading to improved energy distribution and higher energy conservation.

As the WMN size continues to grow to 120, 140, and 160 routers, TTHHO consistently demonstrates higher residual energy values compared to the competing algorithms. For example, with 140 routers, TTHHO achieves 13308.7, while the highest residual energy achieved by SCA is 11552.66. This significant difference highlights TTHHO's capability to create energy-efficient clusters, ultimately contributing to prolonged network operation.

The visual representation of the residual energy is shown in Fig. 10 which also illustrates the comparison between the proposed TTHHO algorithm and other competing optimization techniques in terms of residual energy for different WMN sizes ranging from 60 to 160 routers. The figure's visual representation reinforces the significance of the proposed TTHHO algorithm in addressing energy efficiency concerns in WMNs. The higher residual energy obtained by TTHHO indicates better energy conservation and utilization, making the network more sustainable and resilient to various challenges.

In summary, the numerical comparison and the visual representation reveal that the proposed TTHHO consistently obtains higher residual energy values across all WMN sizes, indicating superior energy efficiency and optimized network structures. TTHHO's ability to strategically place the sink node and routers leads to better energy conservation and network longevity compared to other competing optimization techniques. These results underscore TTHHO's effectiveness and potential in addressing energy-related challenges in WMNs, making it a promising choice for enhancing the performance and sustainability of WMNs in various real-world scenarios.

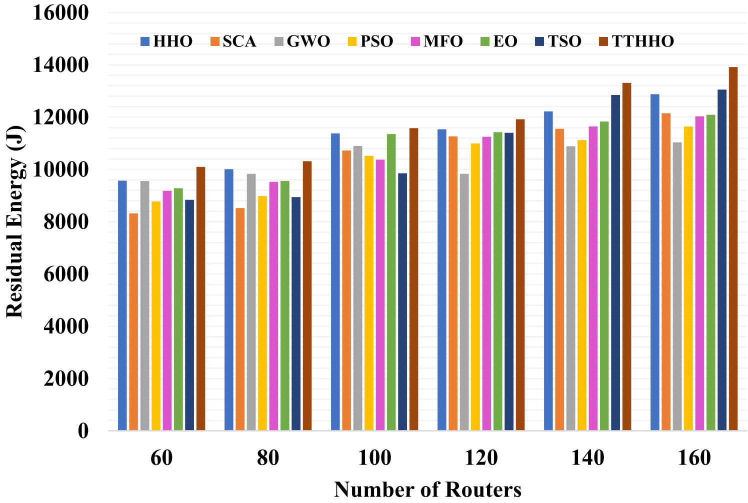

Fig. 10. Residual Energy of TTHHO vs other algorithm for different WMN sizes.

Table 8
Comparison of the proposed TTHHO with the-state-of-the-art.

Ref.	Approach	No. Routers and Clients	Network grid size	Coverage Rate	Connectivity Rate	Remarks
[19]	TS	64 routers and 192 clients	132 × 132	87%	89%	Fair Connectivity and coverage
[38]	PSO	40 routers and 120 clients	1000 × 1000	87%	99%	Fair coverage and high connectivity
[37]	HHO	2000 Routers	1000 × 1000	-	-	Limited to sink node placement
[26]	PSO	64 routers and 192 clients	128 × 128	-	-	-
[18]	MVO	45 routers and 100 clients	2000 × 2000	90%	-	Good connectivity
[3]	HHO	100 routers and 100 clients	1000 × 1000	98%	98%	Good coverage and connectivity
[39]	COA	40 routers and 100 clients	2000 × 2000	80%	93%	Good connectivity and fair coverage
Current Work	TTHHO	62 routers and 100 clients	1000 × 1000	**100%**	**100%**	**Full coverage and connectivity**

4.2.6. Assessments and comparison with the-state-of-the-art

In Table 8, a comprehensive performance comparison and evaluation against state-of-the-art approaches is presented. The table contrasts the effectiveness of the proposed TTHHO algorithm employed in this study with relevant literature, considering key metrics such as network size, number of clients and routers, and coverage and connectivity rates. Notably, despite utilizing a substantial grid, our TTHHO algorithm demonstrates superior performance compared to the state-of-the-art. Specifically, the TTHHO algorithm impressively achieves full coverage and connectivity. Noteworthy is the fact that these high percentages are attained with a reduced number of routers in the network when compared to [19,39,38]. Furthermore, rigorous statistical analyses and simulation results corroborate the superiority of the TTHHO algorithm in terms of network connectivity, coverage, and network reduction. This enhanced performance can be attributed to the thoughtful design phase undertaken by the algorithm's designer.

5. Conclusion

The proposed TTHHO algorithm has emerged as a highly effective and robust solution for optimizing various aspects of WMNs. Through comprehensive evaluations and comparisons with competing algorithms, TTHHO consistently demonstrated superior performance in terms of convergence, coverage, congestion reduction, and optimal sink node placement based on residual energy. Its faster convergence and increased likelihood of reaching global minima in benchmark functions underscore its remarkable optimization capabilities. With congestion reduction rates as high as 61.25% for 160 routers, rapid convergence to 0.003125, and superior residual energy management, TTHHO establishes its supremacy. A key advantage of TTHHO lies in its ability to efficiently utilize residual energy, strategically placing the sink node in areas with higher energy levels. This dynamic sink node placement ensures extended network operational time and enhanced network longevity, promoting sustainability and resilience in the face of challenges. Notably, TTHHO achieves 100% coverage rate for clients while utilizing fewer routers, making it a compelling and resource-efficient solution. The findings collectively support TTHHO's effectiveness in addressing the complexities of WMN design and operation, making it a valuable contribution to the field of wireless communications and network optimization.

In future research, exploring the scalability, robustness, and adaptability of the TTHHO algorithm for larger WMNs and dynamic conditions is recommended. Investigating multi-objective optimization, adaptive parameter tuning, and integration with emerging technologies like 5G and IoT can extend the algorithm's applicability. Additionally, it is important to note a limitation in our current model, which assumes all routers are battery-powered. The presence of non-rechargeable devices, such as sensors, introduces a different energy dynamic that should be addressed in future iterations for a more comprehensive applicability to diverse network environments.

CRediT authorship contribution statement

Hakim Abdulrab: Writing – review & editing, Writing – original draft, Software, Methodology, Formal analysis, Data curation, Conceptualization. **Fawnizu Azmadi Hussin:** Writing – review & editing, Visualization, Supervision. **Idris Ismail:** Writing – review & editing, Investigation, Funding acquisition. **Maher Assad:** Writing – review & editing, Visualization, Funding acquisition, Formal analysis. **Azlan Awang:** Visualization, Investigation, Formal analysis. **Hussein Shutari:** Writing – review & editing, Formal analysis. **Devan Arun:** Writing – review & editing, Methodology, Conceptualization.

Declaration of competing interest

The authors declare that they have no known competing financial interests or personal relationships that could have appeared to influence the work reported in this paper.

Data availability

No additional data associated with this paper.

Acknowledgement

The work in this manuscript was partially supported by Ajman University under Grant 2022-IRG-ENIT-2 and Univesiti Teknologi PETRONAS under YUTP-PRG Cycle 2022 cost centre 015PBC-008.

Appendix A. Supplementary material

Supplementary material related to this article can be found online at https://doi.org/10.1016/j.heliyon.2024.e28719.

References

[1] Q. Wang, W. Li, Z. Yu, Q. Abbasi, M. Imran, S. Ansari, Y. Sambo, L. Wu, Q. Li, T. Zhu, An overview of emergency communication networks, Remote Sens. 15 (6) (2023) 1595.
[2] A. Guerna, S. Bitam, C.T. Calafate, Roadside unit deployment in Internet of vehicles systems: a survey, Sensors 22 (9) (2022) 3190.
[3] H.Q. Abdulrab, F.A. Hussin, A. Abd Aziz, A. Awang, I. Ismail, M.S.M. Saat, H. Shutari, Optimal coverage and connectivity in industrial wireless mesh networks based on Harris' Hawk optimization algorithm, IEEE Access 10 (2022) 51048–51061.
[4] M. Hussain, N. Ahmed, M. Ahmed, Z. Iqubal, N. Sarma, et al., QoS provisioning in wireless mesh networks: a survey, Wirel. Pers. Commun. 122 (1) (2022) 157–195, https://doi.org/10.1007/s11277-021-08893-3.
[5] L.K. Ketshabetswe, A.M. Zungeru, M. Mangwala, J.M. Chuma, B. Sigweni, Communication protocols for wireless sensor networks: a survey and comparison, Heliyon 5 (5) (2019).
[6] J.R. Cotrim, J.H. Kleinschmidt, Lorawan mesh networks: a review and classification of multihop communication, Sensors 20 (15) (2020) 4273.
[7] H. Abdulrab, F.A. Hussin, A. Awang, I. Ismail, P.A.M. Devan, H. Shutari, Optimal node placement and congestion reduction in an industrial wireless mesh network using HHO algorithm, in: 2022 International Conference on Future Trends in Smart Communities (ICFTSC), IEEE, 2022, pp. 164–169.
[8] W. Wang, Deployment and optimization of wireless network node deployment and optimization in smart cities, Comput. Commun. 155 (2020) 117–124.
[9] T.M. Ghazal, M.K. Hasan, H.M. Alzoubi, M. Alshurideh, M. Ahmad, S.S. Akbar, Internet of things connected wireless sensor networks for smart cities, in: The Effect of Information Technology on Business and Marketing Intelligence Systems, Springer, 2023, pp. 1953–1968.
[10] M. Wzorek, C. Berger, P. Doherty, Router and gateway node placement in wireless mesh networks for emergency rescue scenarios, Auton. Intell. Syst. 1 (2021) 1–30.
[11] S.B. Joseph, E.G. Dada, A. Abidemi, D.O. Oyewola, B.M. Khammas, Metaheuristic algorithms for pid controller parameters tuning: review, approaches and open problems, Heliyon 8 (5) (2022) e09399.
[12] K. Reddy, A.K. Saha, A modified whale optimization algorithm for exploitation capability and stability enhancement, Heliyon 8 (10) (2022).
[13] H. Abdulrab, F.A. Hussin, A. Abd Aziz, A. Awang, I. Ismail, P. Devan, Reliable fault tolerant-based multipath routing model for industrial wireless control systems, Appl. Sci. 12 (2) (2022) 544.
[14] P.A.M. Devan, R. Ibrahim, M. Omar, K. Bingi, H. Abdulrab, A novel hybrid Harris hawk-arithmetic optimization algorithm for industrial wireless mesh networks, Sensors 23 (13) (2023) 6224.
[15] M.H. Qais, H.M. Hasanien, S. Alghuwainem, Transient search optimization: a new meta-heuristic optimization algorithm, Appl. Intell. 50 (2020) 3926–3941.
[16] A.A. Heidari, S. Mirjalili, H. Faris, I. Aljarah, M. Mafarja, H. Chen, Harris hawks optimization: algorithm and applications, Future Gener. Comput. Syst. 97 (2019) 849–872.

[17] S. Mirjalili, Sca: a sine cosine algorithm for solving optimization problems, Knowl.-Based Syst. 96 (2016) 120–133.
[18] L.H. Binh, T.K. Truong, An efficient method for solving router placement problem in wireless mesh networks using multi-verse optimizer algorithm, Sensors 22 (15) (2022) 5494, https://doi.org/10.3390/s22155494.
[19] F. Xhafa, C. Sánchez, A. Barolli, M. Takizawa, Solving mesh router nodes placement problem in wireless mesh networks by tabu search algorithm, J. Comput. Syst. Sci. 81 (8) (2015) 1417–1428, https://doi.org/10.1016/j.jcss.2014.12.018.
[20] C.-C. Lin, L. Shu, D.-J. Deng, Router node placement with service priority in wireless mesh networks using simulated annealing with momentum terms, IEEE Syst. J. 10 (4) (2016) 1402–1411, https://doi.org/10.1109/JSYST.2014.2341033.
[21] A. Barooli, S. Sakamoto, L. Barolli, M. Takizawa, Performance evaluation of WMN-PSODGA system for node placement problem in WMNs considering four different crossover methods, in: 2018 IEEE 32nd International Conference on Advanced Information Networking and Applications (AINA), 2018, pp. 850–857.
[22] S. Sakamoto, K. Ozera, M. Ikeda, L. Barolli, Implementation of intelligent hybrid systems for node placement problem in WMNs considering particle swarm optimization, hill climbing and simulated annealing, Mob. Netw. Appl. 23 (1) (2018) 27–33, https://doi.org/10.1007/s11036-017-0897-7.
[23] S. Sakamoto, E. Kulla, T. Oda, M. Ikeda, L. Barolli, F. Xhafa, A simulation system for WMN based on SA: performance evaluation for different instances and starting temperature values, Int. J. Space-Based Situat. Comput. 4 (3–4) (2014) 209–216.
[24] T. Oda, Y. Liu, S. Sakamoto, D. Elmazi, L. Barolli, F. Xhafa, Analysis of mesh router placement in wireless mesh networks using Friedman test considering different meta-heuristics, Int. J. Commun. Netw. Distrib. Syst. 15 (1) (2015) 84–106.
[25] C.-C. Lin, Dynamic router node placement in wireless mesh networks: a pso approach with constriction coefficient and its convergence analysis, Inf. Sci. 232 (2013) 294–308, https://doi.org/10.1016/j.ins.2012.12.023.
[26] C.-C. Lin, P.-T. Tseng, T.-Y. Wu, D.-J. Deng, Social-aware dynamic router node placement in wireless mesh networks, Wirel. Netw. 22 (4) (2016) 1235–1250, https://doi.org/10.1007/s11276-015-1036-7.
[27] C.-C. Lin, Y.-S. Li, D.-J. Deng, A bat-inspired algorithm for router node placement with weighted clients in wireless mesh networks, in: 9th International Conference on Communications and Networking in China, IEEE, 2014, pp. 139–143.
[28] L. Sayad, L. Bouallouche-Medjkoune, D. Aissani, An electromagnetism-like mechanism algorithm for the router node placement in wireless mesh networks, Soft Comput. 23 (12) (2019) 4407–4419, https://doi.org/10.1007/s00500-018-3096-y.
[29] N. Chouhan, U.R. Bhatt, R. Upadhyay, V. Bhat, FiWi network planning for WiFi enabled gram panchayats of India: a frame work using component placement optimization, Opt. Fiber Technol. 76 (2023) 103242.
[30] N. Chouhan, U.R. Bhatt, R. Upadhyay, Weighted Salp Swarm and Salp Swarm algorithms in FiWi access network: a new paradigm for onu placement, Opt. Fiber Technol. 63 (2021) 102505.
[31] H. Emami, M.M. Alipour, Chaotic local search-based Levy flight distribution algorithm for optimizing onu placement in fiber-wireless access network, Opt. Fiber Technol. 67 (2021) 102733.
[32] H. Emami, Onu placement in fiwi network using enhanced backtracking search algorithm, in: 2022 4th West Asian Symposium on Optical and Millimeter-Wave Wireless Communications (WASOWC), IEEE, 2022, pp. 01–06.
[33] P. Singh, S. Prakash, Implementation of Marin predators algorithm for optimizing the position of multiple optical network units in fiber wireless access networks, Opt. Fiber Technol. 72 (2022) 102971.
[34] P. Singh, S. Prakash, Optical network unit placement in fiber-wireless (fiwi) access network by whale optimization algorithm, Opt. Fiber Technol. 52 (2019) 101965, https://doi.org/10.1016/j.yofte.2019.101965.
[35] G.P. Gupta, S. Jha, Biogeography-based optimization scheme for solving the coverage and connected node placement problem for wireless sensor networks, Wirel. Netw. 25 (6) (2019) 3167–3177, https://doi.org/10.1007/s11276-018-1709-0.
[36] J.L.K.E. Fendji, C. Thron, A simulated annealing based centre of mass (sac) approach for mesh routers placement in rural areas, Int. J. Oper. Res. Inf. Syst. 11 (1) (2020) 37–65, https://doi.org/10.4018/IJORIS.2020010102.
[37] E.H. Houssein, M.R. Saad, K. Hussain, W. Zhu, H. Shaban, M. Hassaballah, Optimal sink node placement in large scale wireless sensor networks based on Harris' Hawk optimization algorithm, IEEE Access 8 (99) (2020) 19381–19397.
[38] N.A. Nouri, Z. Aliouat, A. Naouri, S.A. Hassak, Accelerated PSO algorithm applied to clients coverage and routers connectivity in wireless mesh networks, J. Ambient Intell. Humaniz. Comput. (2021) 1–15, https://doi.org/10.1007/s12652-021-03283-w.
[39] S.M. Taleb, Y. Meraihi, A.B. Gabis, S. Mirjalili, A. Zaguia, A. Ramdane-Cherif, Solving the mesh router nodes placement in wireless mesh networks using coyote optimization algorithm, IEEE Access 10 (2022) 52744–52759, https://doi.org/10.1109/ACCESS.2022.3166866.
[40] K. Nitesh, P.K. Jana, Relay node placement with assured coverage and connectivity: a Jarvis March approach, Wirel. Pers. Commun. 98 (1) (2018) 1361–1381, https://doi.org/10.1007/s11277-017-4922-8.
[41] S. Sapre, S. Mini, Optimized relay nodes positioning to achieve full connectivity in wireless sensor networks, Wirel. Pers. Commun. 99 (4) (2018) 1521–1540, https://doi.org/10.1007/s11277-018-5290-8.
[42] N. Neggaz, A.A. Ewees, M. Abd Elaziz, M. Mafarja, Boosting salp swarm algorithm by sine cosine algorithm and disrupt operator for feature selection, Expert Syst. Appl. 145 (2020) 113103.
[43] H. Shutari, N. Saad, N.B.M. Nor, M.F.N. Tajuddin, A. Alqushaibi, M.A. Magzoub, Towards enhancing the performance of grid-tied VSWT via adopting sine cosine algorithm-based optimal control scheme, IEEE Access 9 (2021) 139074–139088.
[44] H. Shutari, T. Ibrahim, N.B.M. Nor, N. Saad, M.F.N. Tajuddin, H.Q. Abdulrab, Development of a novel efficient maximum power extraction technique for grid-tied vswt system, IEEE Access 10 (2022) 101922–101935.
[45] A. Alqushaibi, S.J. Abdulkadir, H.M. Rais, Q. Al-Tashi, M.G. Ragab, H. Alhussian, Enhanced weight-optimized recurrent neural networks based on sine cosine algorithm for wave height prediction, J. Mar. Sci. Eng. 9 (5) (2021) 524.
[46] H. Shutari, T. Ibrahim, N.B.M. Nor, H. Abdulrab, N. Saad, Q. Al-Tashi, Coordination of enhanced control schemes for optimal operation and ancillary services of grid-tied vswt system, IEEE Access 11 (2023) 43520–43535.
[47] P.A.M. Devan, F.A. Hussin, R.B. Ibrahim, K. Bingi, M. Nagarajapandian, M. Assaad, An arithmetic-trigonometric optimization algorithm with application for control of real-time pressure process plant, Sensors 22 (2) (2022) 617.
[48] H.Q. Abdulrab, F.A. Hussin, I. Ismail, M. Assaad, A. Awang, H. Shutari, P.A.M. Devan, Hybrid Harris Hawks with sine cosine for optimal node placement and congestion reduction in an industrial wireless mesh network, IEEE Access 11 (2023) 2500–2523.